Réunions AstroDoc

Le Dictionnaire de Nomenclature

07/12/2017

Equipe Dictionnaire

« *During the last decade or so, the naming of astronomical objects has become a nightmare, due in part to the opening up of the electromagnetic spectrum for exploration by satellites and to the improved resolution of ground-based observations in the infrared and radio part of the spectrum.* »

Lortet & Dickel, 1984A&AS...56....1L

"Tricks and traps in astronomical nomenclature"

- Le Dictionnaire de Nomenclature en quelques mots
- La création d'acronymes :
  - quelques définitions
  - au cœur d'un ensemble d'étapes
- En pratique

Le Dictionnaire de Nomenclature

- Un guide pour se repérer dans les nomenclatures utilisées pour identifier les objets astronomiques (en dehors du Système solaire)

- Discussion à l'Assemblée Générale de l'UAI de 1979 => publication du premier Dictionnaire en 1983 *(Fernandez, Lortet & Spite, 1983A&AS...52....1F)*

- 1994 : deuxième édition du Dictionnaire, accompagnée du lancement d'une version en ligne – avec les commandes "`info [-l] cati acro`", "`info [-l] cat word`", etc *(Lortet, Borde & Ochsenbein, 1994A&AS..107..193L)*

La création d'acronymes

- Nouveaux acronymes pour :
  - les objets nouvellement découverts,
  - les observations à des longueurs d'onde différentes,
  - les observations à des résolutions différentes
- Désignation = Acronyme + Format
  - pas toujours claires, pas toujours uniques
  - parfois une désignation spécifique est utilisée, parfois non…
- Le Dictionnaire recense ces désignations (au mieux…)

Le choix des acronymes

- L'acronyme utilisé par les auteurs est prioritaire s'il est "correct" pour nous, c'est-à-dire :
  - s'il n'existe pas déjà dans le Dictionnaire
  - s'il ne s'agit pas d'un type d'objet ou du nom d'un télescope ou d'un instrument
  - si l'acronyme proposé n'est pas trop simple (1 ou 2 lettres seulement) ou ambigu

- Sinon on crée un acronyme entre crochets : [AAAYYYY]
  AAA : initiales des 1 à 3 premiers auteurs
  YYYY : année de publication

Les formats

- Coller au maximum à ce qui est publié, tout en essayant de respecter les recommandations de l'UAI et de prendre en compte les besoins pour SIMBAD

- Principaux problèmes rencontrés :
  - pas de format du tout
  - J (de J2000) omis
  - ambiguïté du format (entre deux tables, voire dans une seule)
  - ...

2 Typical formats (usual or recommended)

Format	Example	Remarks
Running number		
NNN...	HD	
Declination zone		
+DD NNN	BD-28 2411	
	Sk-69 72	Not Sk72-69
Equatorial coordinates		
HHMM+DD	PKS	
HHMM+DDd	PKS	
BHHMM+DD	PSR	
BHHMM+DDd	PKS	
JHHMM+DDMM	PSR	
	PKS	
HHMMm+DDMM	IRAS	Point Source Cat.
HHMM.m+DDMM	1E	(IPC)
HHMMSS+DDMMSS	6C	
HHMMSS.s+DDMMSS	1E	(HRI)
BHHMMSS.s+DDMMSS	6C	
Galactic coordinates		
LLL.ℓ+BB.b+VVV	HVC	
GLLL.ℓ+BB.b	PN	
Field		
FFF-NNNN	LP	hyphens are recommended
	ESO	
FFFF-NNNNN	GSC	
Constellation		
CCC YYYY	Nova	
Year or Date		
YYYYA	SN 1987A	
YYYYaa	SN 1993aj	
YYMMDDA	GRB 991216	γ-ray burst
YYYY MMM DDA	GB 1979 Nov 05A	

http://cdsarc.u-strasbg.fr/vizier/Dic/iau-spec.htx

Un ensemble complexe d'étapes

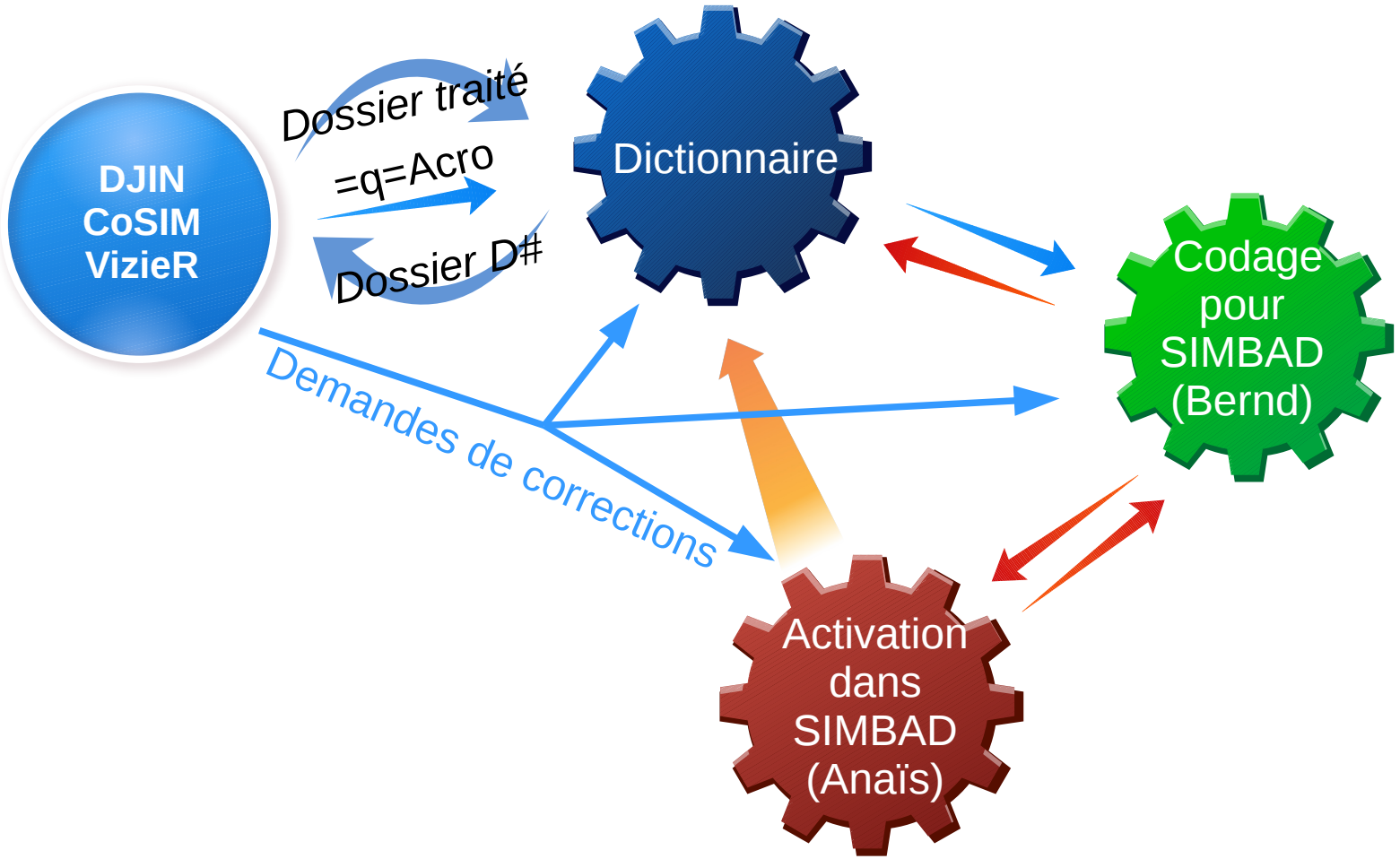

3. La création d'un acronyme en pratique

- Cas des =q=Acro ou =q=AAcro
- Rapide première analyse du contexte d'utilisation des identificateurs posant problème
  - Lire le commentaire de travail
  - Lire l'abstract
  - Voir rapidement les noms concernés en contexte (utiliser DJIN peut aider)
  - => Décision : acronyme ou non ?
    - Si non : mettre à jour le commentaire de travail dans SIMBAD (objets déjà connus ; crossids suffisantes ; pas des objets ; ...)
    - Si besoin : consulter un astronome (pour vérifier si ce sont bien des objets par exemple)
    - Parfois : mettre en attente (par ex. de parution d'un article plus clair)
    - Dans tous les cas : vérifier si d'autres références sont concernées par cette réponse

- Si oui, pour quelle référence ?
  La recherche de la référence d'origine peut être compliquée
  - Il faut parfois remonter le fil des références citées, parfois en passant par des sites web de projets...
  - L'échantillon étudié semble venir d'ailleurs
  - Un numéro discontinu peut indiquer une liste complète préalablement publiée (ou pas...)
  - Parfois, on reconnaît des noms d'auteurs ou des formats
  - Souvent on détecte des références liées (=> bien mettre à jour les commentaires de travail dans SIMBAD pour un effet domino efficace une fois l'acronyme créé)

- Les informations nécessaires pour compléter le Dictionnaire :
  - Les auteurs utilisent-ils un acronyme ?
  - Le(s) instrument(s) utilisé(s)
  - Le nombre d'identificateurs concernés par l'acronyme (sans forcément tenir compte des doublons)
  - Le type d'objet (de l'article et celui pour SIMBAD)
  - ...

- => Analyse plus détaillée de la référence d'origine :
  - Section Observations
  - Citations de la table dans le texte
  - Les occurrences en contexte
  - ...

- Des informations peuvent être utiles à la mise à jour de SIMBAD ?
  - => compléter le commentaire de travail

Le cas idéal : 2017ApJS..231...16J

=q=Acro Tables 3-5: IMS JHHMMSS.ss+DDMMSS.s
= IMS JHHMM+DDMM: NL. -MN-24.08.14

Portal Simbad VizieR Aladin X-Match Other Help

Dictionary of Nomenclature of Celestial Objects

Details on Acronym: **IMS**

IMS (Infrared Medium-deep Survey) *(Not yet in Simbad)*

Write: <<**IMS** JHHMMSS.ss+DDMMSS.s>>
<<**IMS** JHHMM+DDMM>> (not recognised by Simbad, but found in literature)

N: 1+6

Object: QSO (SIMBAD class: QSO = Quasar)

Note: The Infrared Medium-deep Survey (IMS) is a moderately wide (120 square degrees) and moderately deep (J~22.5-23mag) NIR imaging survey with UKIRT WFCAM.
The IMS includes seven extragalactic fields (XMM-LSS, CFHTLS-W2, Lockman Hole, EGS, ELAIS-N1, ELAIS-N2, and SA22).

in source: NAME XMM-LSS Field

in source: NAME Lockman Hole

in source: NAME Extended Groth Strip

in source: ELAIS N1

in source: ELAIS N2

in source: SSA 22

Ref: =2015ApJ...813L..35K

by KIM Y. , IM M., JEON Y., KIM M., CHOI C., HONG J., HYUN M., JUN H.D., KAROUZOS M., KIM D., KIM D., KIM J.-W., KIM J.H., LEE S.-K., PAK S., PARK W.-K., TAAK Y.C., YOON Y.

Astrophys. J., 813, L35 (2015)

Discovery of a faint quasar at z ~ 6 and implications for cosmic reionization.

- Figs 2-3, Table 1: <IMS JHHMMSS.ss+DDMMSS.s> N=1.

Ref: =2017ApJS..231...16J

by JEON Y. , IM M., KIM D., KIM Y., JUN H.D., PAK S., TAAK Y.C., BAEK G., CHOI C., CHOI N., HONG J., HYUN M., JI T.-G., KAROUZOS M., KIM D., KIM J.-W., KIM J.H., KIM M., KIM S., LEE H.-I., LEE S.-K., PARK W.-K., PARK W., YOON Y.

Astrophys. J., Suppl. Ser., 231, 16-16 (2017)

The Infrared Medium-deep Survey. III. Survey of luminous quasars at 4.7 <= z <= 5.4.

- Table 3: <IMS JHHMMSS.ss+DDMMSS.s> N=6.

Origin of the Acronym: **A** = *Assigned by the author(s)*

Table 3
General Information of IMS Quasars

Name	R.A. and Decl. (J2000.0)	Redshift	M_{1450}
IMS J032407.70+042613.3	03:24:07.70 + 04:26:13.3	4.70(Lyα)[a], 4.68(C IV), 4.73(Mg II)	−27.21 ± 0.29
IMS J012247.33+121623.9	01:22:47.33 + 12:16:23.9	4.83(Lyα)[b], 4.81(C IV)	−26.47 ± 0.68
IMS J143704.82+070808.3	14:37:04.82 + 07:08:08.3	4.94(Lyα)[c]	−27.14 ± 0.09
IMS J222514.39+033012.6	22:25:14.39 + 03:30:12.6	5.35(Lyα)[d], 5.26(Mg II)	−26.47 ± 0.29
IMS J102201.90+080122.2	10:22:01.90 + 08:01:22.2	5.36(Lyα)	−27.38 ± 0.10
IMS J015533.28+041506.8	01:55:33.28 + 04:15:06.8	5.35(Lyα)[e], 5.27(C IV)	−26.85 ± 1.09

Notes. z_{spec} from other papers are all derived from Lyα.
[a] z_{spec} = 4.72 from Wang et al. (2016).
[b] z_{spec} = 4.76 from Yi et al. (2015) and z_{spec} = 4.79 from Wang et al. (2016).
[c] z_{spec} = 4.93 from Wang et al. (2016).
[d] z_{spec} = 5.24 from Wang et al. (2016).
[e] z_{spec} = 5.37 from Wang et al. (2016).

observed for the flux calibration. The slit widths varied from 1.″0 to 3.″0, depending on the seeing conditions. Table 2 shows the summary of the optical spectroscopic observations of the discovered quasars, namely the total integration time and the slit width for each target.

We followed the typical steps for preprocessing, including bias subtraction, dark subtraction, and flat fielding, for each science image, standard star image, and arc image, using the `noao.imred.ccdred` package in IRAF. The spectra were extracted using the `noao.imred.kpnoslit` or the `noao.twodspec.apextract` packages in IRAF for each single image. We used an optimal aperture size for each image where the S/N is highest. After this, wavelength and flux calibrations were conducted. The spectra were flux-calibrated using spectra of the standard stars. Considering the light loss due to variable seeing conditions, we scaled the spectra using broadband photometry. We chose *i*-band for this calibration because we get the highest S/N in this band for the observed spectra. The flux-calibrated spectra were combined in median, using the `scombine` task of IRAF, then corrected for Galactic extinction using values from Cardelli et al. (1989) and Schlegel et al. (1998).

We observed 47 candidates, six of which turned out to be high-redshift quasars at $4.7 \leqslant z \leqslant 5.4$, referred to as Infrared Medium-deep Survey (IMS) quasars. Table 3 lists the names, coordinates, and redshifts (Section 3.2) of the six quasars. The naming convention of our quasars is IMS JHHMMSS.SS ± DDMMSS.S in J2000.0 coordinates (IMS JHHMM ± DDMM for brevity).

2.4. NIR Spectroscopic Observation

To measure their black hole masses and Eddington ratios, we observed four of the six newly discovered quasars with the Folded-port InfraRed Echellette (FIRE[13]) spectrograph on the *Magellan* telescope (IMS J0324+0426, IMS J0122+1216, and IMS J0155+0415), as well as with the Gemini Near Infra-Red Spectrograph (GNIRS) on the Gemini North (Gemini-N) telescope (IMS J2225+0330; program GN-2015B-Q-77). Table 2 shows the summary of our *Magellan* and Gemini-N observations.

In the *Magellan*/FIRE observation, we used a slit width of 1.″00 with the Echelle mode ($R = 3600$). The ABBA pointing method was used for the sky subtraction between exposures. We observed standard stars for each target. Data for the flat fielding and wavelength calibration were also taken. The data reduction was conducted using the IDL suite `FIREHOSE`. This pipeline conducts the preprocessing, object extraction, telluric correction, flux calibration, and spectra combining.

In the Gemini-N/GNIRS observation, we used the cross-dispersed (XD) mode with a 32 line mm^{-1} grating, short blue camera, and its SXD prism. Adopting a slit of 0.″675 width, we

[13] http://web.mit.edu/~rsimcoe/www/FIRE/index.html

Un cas plus compliqué : 2017ApJ...837...89W

=q=Acro
Table 2: GLASS NNNNN: NL.

SIMBAD references

other query modes : Identifier query | Coordinate query | Criteria query | Reference query | Basic query | Script submission | TAP | Output options | Help

Reference query: 2017ApJ...837...89W (1 found) C.D.S. - SIMBAD4 rel 1.5.12 - 2017.12.06CET16:09:12

2017ApJ...837...89W *- Astrophys. J., 837, 89-89 (2017) - 21.03.17 24.10.17 March(I) 2017 2017-03-01*

The Grism Lens-Amplified Survey from Space (GLASS). X. Sub-kiloparsec resolution gas-phase metallicity maps at cosmic noon behind the Hubble Frontier Fields cluster MACS1149.6+2223.

WANG X.; JONES T.A.; TREU T.; MORISHITA T.; ABRAMSON L.E.; BRAMMER G.B.; HUANG K.-H.; MALKAN M.A.; SCHMIDT K.B.; FONTANA A.; GRILLO C.; HENRY A.L.; KARMAN W.; KELLY P.L.; MASON C.A.; MERCURIO A.; ROSATI P.; SHARON K.; TRENTI M.; VULCANI B.

Abstract (from CDS): We combine deep Hubble Space Telescope grism spectroscopy with a new Bayesian method to derive maps of gas-phase metallicity for 10 star-forming galaxies at high redshift (1.2 z 2.3). Exploiting lensing magnification by the foreground cluster MACS1149.6+2223, we reach sub-kiloparsec spatial resolution and push the limit of stellar mass associated with such high-z spatially resolved measurements below 10^8 $M_\odot$ for the first time. Our maps exhibit diverse morphologies, indicative of various effects such as efficient radial mixing from tidal torques, rapid accretion of low-metallicity gas, and other physical processes that can affect the gas and metallicity distributions in individual galaxies. Based upon an exhaustive sample of all existing sub-kiloparesec resolution metallicity gradient measurements at high z, we find that predictions given by analytical chemical evolution models assuming a relatively extended star-formation profile in the early disk-formation phase can explain the majority of observed metallicity gradients, without involving galactic feedback or radial outflows. We observe a tentative correlation between stellar mass and metallicity gradients, consistent with the "downsizing" galaxy formation picture that more massive galaxies are more evolved into a later phase of disk growth, where they experience more coherent mass assembly at all radii and thus show shallower metallicity gradients. In addition to the spatially resolved analysis, we compile a sample of homogeneously cross-calibrated integrated metallicity measurements spanning three orders of magnitude in stellar mass at z ~ 1.8. We use this sample to study the mass-metallicity relation (MZR) and find that the slope of the observed MZR can rule out the momentum-driven wind model at a 3σ confidence level.

Journal keyword(s): galaxies: abundances - galaxies: evolution - galaxies: formation - galaxies: high-redshift - gravitational lensing: strong

Status in Simbad: being processed

Simbad objects: 16

Commentaire privé:

(q)Laurent Table 2: On prend dans SIMBAD? Si oui quelles DF? Demande d'acronyme? -MN-19.04.17
// (T)Magali =q=Acro Table 2: GLASS NNNNN: NL. (otype: gal, J2000 (opt) C, mag H (AB) [~] D, redshift zs [~] (opt)) -MN-05.05.17

The Astrophysical Journal, 837:89 (28pp), 2017 March 1 https://doi.org/10.3847/1538-4357/aa603c

Titre+Abstract

The Grism Lens-Amplified Survey from Space (GLASS). X. Sub-kiloparsec Resolution Gas-phase Metallicity Maps at Cosmic Noon behind the Hubble Frontier Fields Cluster MACS1149.6+2223

Xin Wang[1], Tucker A. Jones[2,3,18], Tommaso Treu[1], Takahiro Morishita[1,4,5], Louis E. Abramson[1], Gabriel B. Brammer[6], Kuang-Han Huang[3], Matthew A. Malkan[1], Kasper B. Schmidt[7], Adriano Fontana[8], Claudio Grillo[9,10], Alaina L. Henry[6,11], Wouter Karman[12], Patrick L. Kelly[13], Charlotte A. Mason[1], Amata Mercurio[14], Piero Rosati[15], Keren Sharon[16], Michele Trenti[17], and Benedetta Vulcani[17]

[1] Department of Physics and Astronomy, University of California, Los Angeles, CA 90095-1547, USA; xwang@astro.ucla.edu
[2] Institute of Astronomy, University of Hawaii, 2680 Woodlawn Drive, Honolulu, HI 96822, USA
[3] University of California Davis, 1 Shields Avenue, Davis, CA 95616, USA
[4] Astronomical Institute, Tohoku University, Aramaki, Aoba, Sendai 980-8578, Japan
[5] Institute for International Advanced Research and Education, Tohoku University, Aramaki, Aoba, Sendai 980-8578, Japan
[6] Space Telescope Science Institute, 3700 San Martin Drive, Baltimore, MD 21218, USA
[7] Leibniz-Institut für Astrophysik Potsdam (AIP), An der Sternwarte 16, D-14482 Potsdam, Germany
[8] INAF—Osservatorio Astronomico di Roma Via Frascati 33—I-00040 Monte Porzio Catone, Italy
[9] Dipartimento di Fisica, Università degli Studi di Milano, via Celoria 16, I-20133 Milano, Italy
[10] Dark Cosmology Centre, Niels Bohr Institute, University of Copenhagen, Juliane Maries Vej 30, DK-2100 Copenhagen, Denmark
[11] Astrophysics Science Division, Goddard Space Flight Center, Code 665, Greenbelt, MD 20771, USA
[12] Kapteyn Astronomical Institute, University of Groningen, Postbus 800, 9700 AV Groningen, The Netherlands
[13] Department of Astronomy, University of California, Berkeley, CA 94720-3411, USA
[14] INAF—Osservatorio Astronomico di Capodimonte, Via Moiariello 16, I-80131 Napoli, Italy
[15] Dipartimento di Fisica e Scienze della Terra, Università degli Studi di Ferrara, via Saragat 1, I-44122 Ferrara, Italy
[16] Department of Astronomy, University of Michigan, 1085 S. University Avenue, Ann Arbor, MI 48109, USA
[17] School of Physics, University of Melbourne, VIC 3010, Australia
Received 2016 October 24; revised 2017 February 8; accepted 2017 February 10; published 2017 March 7

Abstract

We combine deep *Hubble Space Telescope* grism spectroscopy with a new Bayesian method to derive maps of gas-phase metallicity for 10 star-forming galaxies at high redshift ($1.2 \lesssim z \lesssim 2.3$). Exploiting lensing magnification by the foreground cluster MACS1149.6+2223, we reach sub-kiloparsec spatial resolution and push the limit of stellar mass associated with such high-z spatially resolved measurements below $10^8\,M_\odot$ for the first time. Our maps exhibit diverse morphologies, indicative of various effects such as efficient radial mixing from tidal torques, rapid accretion of low-metallicity gas, and other physical processes that can affect the gas and metallicity distributions in individual

Table 2
Global Demographic Properties of the Metallicity Gradient Sample Analyzed in This Work

ID	R.A. (deg.)	Decl. (deg.)	z_{spec}	μ[a]	H_{160} Magnitude (ABmag)	SED Fitting		
						$\log(M_*{}^{b}/M_\odot)$	A_V^{Sc}	$12+\log(O/H)$
01422	177.398643	22.387499	2.28	2.35 [2.09, 2.26]	24.46	$9.29^{+0.07}_{-0.01}$	<0.01	$8.26^{+0.11}_{-0.13}$
02389	177.406546	22.392860	1.89	43.25 [37.47, 50.28]	23.29	$8.43^{+0.06}_{-0.07}$	<0.01	$7.88^{+0.16}_{-0.15}$
02607[d]	177.413454	22.393843	1.86	3.01 [2.79, 2.98]	22.63	$10.25^{+0.06}_{-0.10}$	$1.70^{+0.42}_{-0.18}$	$7.70^{+0.13}_{-0.11}$
02806	177.392541	22.394921	1.50	4.82 [3.11, 3.51]	23.35	$8.72^{+0.19}_{-0.01}$	$0.50^{+0.01}_{-0.01}$	$7.96^{+0.15}_{-0.16}$
02918	177.412652	22.395723	1.78	2.95 [2.72, 2.91]	25.22	$8.37^{+0.15}_{-0.08}$	$0.10^{+0.34}_{-0.10}$	$8.42^{+0.11}_{-0.14}$
03746	177.391848	22.400105	1.25	3.78 [3.56, 3.83]	22.48	$8.81^{+0.03}_{-0.01}$	<0.01	$8.11^{+0.10}_{-0.11}$
04054	177.403393	22.402456	1.49	3.39 [3.04, 3.28]	21.27	$9.64^{+0.05}_{-0.01}$	$1.10^{+0.01}_{-0.01}$	$8.70^{+0.09}_{-0.11}$
05422	177.382077	22.407510	1.97	3.63 [3.11, 4.41]	25.05	$8.45^{+0.15}_{-0.46}$	$0.00^{+0.56}_{-0.01}$	$7.56^{+0.16}_{-0.12}$
05709	177.397234	22.406181	1.68	7.10 [6.74, 7.53]	25.44	$7.90^{+0.02}_{-0.03}$	<0.01	$8.21^{+0.13}_{-0.21}$
05732	177.415126	22.406195	1.68	1.56 [1.51, 1.61]	23.45	$9.09^{+0.01}_{-0.01}$	<0.01	$8.41^{+0.10}_{-0.12}$
05811	177.389220	22.407583	2.31	7.50 [6.88, 9.34]	23.79	$8.85^{+0.11}_{-0.10}$	<0.01	$8.16^{+0.14}_{-0.21}$
05968	177.406922	22.407499	1.48	1.84 [1.78, 1.96]	22.24	$9.34^{+0.02}_{-0.03}$	$0.60^{+0.20}_{-0.01}$	$8.47^{+0.07}_{-0.08}$
07058	177.405976	22.412977	1.79	2.13 [1.97, 3.01]	24.28	$8.74^{+0.17}_{-0.15}$	$0.00^{+0.12}_{-0.01}$	$8.38^{+0.13}_{-0.19}$
07255	177.385990	22.414074	1.27	2.34 [2.31, 2.99]	22.47	$9.36^{+0.01}_{-0.21}$	$0.30^{+0.21}_{-0.01}$	$8.38^{+0.08}_{-0.08}$

Notes. The error bars and upper/lower limits shown in the columns of SED fitting and EL diagnostics correspond to 1σ confidence r
SED fitting results do not include any systematic uncertainties associated with the Bruzual & Charlot (2003) stellar population mo
[a] Best-fit magnification values and 1σ confidence intervals. Except for galaxy ID 02389, the magnification results are from the GLAFI
the HFF interactive online magnification calculator available at https://archive.stsci.edu/prepds/frontier/lensmodels/webtool/magn
use the Sharon & Johnson version 3 model instead to compute the magnification results and correct for lensing magnification.
[b] Values presented here are corrected for lensing magnification.
[c] The superscripts of "S" and "N" refer to the stellar and nebular V-band dust extinction in units of magnitude, respectively.
[d] The EL diagnostic result on this source is not trustworthy, since it is classified as an AGN candidate (see Section 5).

3729 := [O II], [O III] λ5008 := [O III], [N II] λ6585 := [N II], [S II] $\lambda\lambda$6718, 6732 := [S II] in this paper.[20]

2. Spectroscopic Data and Sample Selection

In Section 2.1, we summarize our *HST* grism observations, data quality, and data reduction. Our sample selection criteria are then described in Section 2.2. We also carried out some ground-based IFU observations on part of our sample, which are presented in Appendix A.

2.1. Hubble Space Telescope Grism Spectroscopy

2.1.1. The Grism Lens-Amplified Survey from Space

The Grism Lens-Amplified Survey from Space[21] (GLASS; Proposal ID 13459; P.I. Treu, Schmidt et al. 2014; Treu et al. 2015) is an *HST* cycle 21 large general observing (GO) program. GLASS observed 10 massive galaxy clusters with the Wide Field Camera 3 Infrared (WFC3/IR) grisms (G102 and 4 orbits per cluster, respectively) targeted at and the Advanced Camera for Survey (ACS)

2.2. Sample Selection

The selection of our metallicity gradient sample is based upon the master redshift catalog for[23] MACS1149.6+2223, published by the GLASS collaboration. As described by Treu et al. (2016), redshifts were determined by combining spectroscopic information from GLASS and the SN Refsdal follow-up *HST* grism programs, ground-based *MUSE* observations and Keck *DEIMOS* data.

For the purpose of this study, we compiled an exhaustive list of spatially extended sources with secure spectroscopic redshift measurements in the range of $z \in [1.2, 2.3]$, showing strong ELs (primarily [O III] and Hβ) in the 2D grism spectra. The reason this redshift range is selected is that we require high signal-to-noise ratio (S/N) detections of [O III], Hβ, and [O II] ELs in the spectra region where grism sensitivity and throughput do not drop significantly, in order to deliver reliable metallicity estimates from well-calibrated EL diagnostics.[24] The selection results in a sample of 14 galaxies.

[23] Available at https://archive.stsci.edu/prepds/glass/.
[24] The Hα EL is only accessible in sources at $z \lesssim 1.5$ in our sample. The GLASS spectra of an exemplary galaxy whose Hα is covered are displayed in Appendix B.

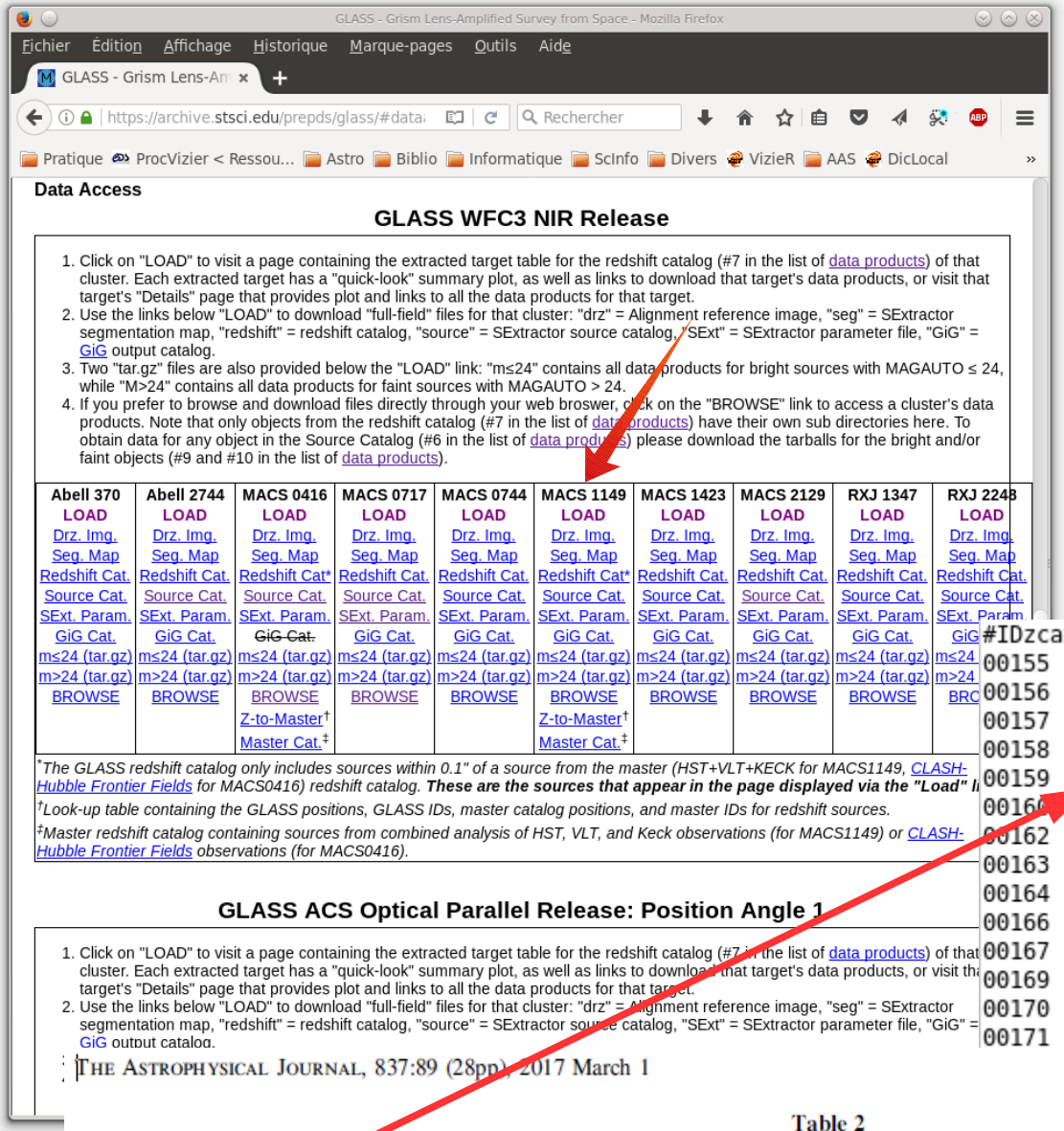

Télécharger les fichiers concernés
Et essayer de retrouver un numéro de la table publiée...

#IDzcat	IDGLASSv001	RA	DEC	redshift	quality	source	
00155	01417	177.413454	22.393843	1.8615	3	1	#
00156	01419	177.416597	22.393925	0.9603	3	1	#
00157	01439	177.390414	22.393626	1.5929	3	1	#
00158	01390	177.408021	22.394379	1.1157	3	1	#
00159	01422	177.386689	22.393877	1.2396	3	1	#
00160	01423	177.400055	22.393902	1.2329	3	1	# 13.3
00162	01305	177.387246	22.394232	2.3195	4	1	#
00163	01301	177.387813	22.395395	0.5432	3	1	#
00164	01414	177.410473	22.394124	1.7084	3	1	#
00166	01388	177.408749	22.394475	2.3189	3	1	# 200.1
00167	01373	177.409808	22.394625	1.2455	3	1	#
00169	01322	177.392541	22.394921	1.4890	3	3	#
00170	01365	177.407378	22.394796	0.5460	4	3	#
00171	00950	177.399831	22.397253	0.5600	4	3	#

Table 2
Global Demographic Properties of the Metallicity Gradient Sample Analyzed in This Work

ID	R.A. (deg.)	Decl. (deg.)	z_{spec}	μ[a]	H_{160} Magnitude (ABmag)	SED Fitting		EL Diagnostics		
						$\log(M_*$[b]$/M_\odot)$	A_V^{Sc}	$12+\log(O/H)$	SFR[b] $[M_\odot\,yr^{-1}]$	A_V^{Nc}
01422	177.398643	22.387499	2.28	2.35 [2.09, 2.26]	24.46	$9.29^{+0.07}_{-0.01}$	<0.01	$8.26^{+0.11}_{-0.13}$	$15.10^{+16.76}_{-7.11}$	<1.07
02389	177.406546	22.392860	1.89	43.25 [37.47, 50.28]	23.29	$8.43^{+0.06}_{-0.07}$	<0.01	$7.88^{+0.16}_{-0.15}$	<6.37	$1.36^{+0.69}_{-0.82}$
02607[d]	177.413454	22.393843	1.86	3.01 [2.79, 2.98]	22.63	$10.25^{+0.06}_{-0.10}$	$1.70^{+0.42}_{-0.18}$	$7.70^{+0.13}_{-0.11}$	>36.51	$2.26^{+0.31}_{-0.58}$
02806	177.392541	22.394921	1.50	4.82 [3.11, 3.51]	23.35	$8.72^{+0.19}_{-0.01}$	$0.50^{+0.01}_{-0.01}$	$7.96^{+0.15}_{-0.16}$	$1.96^{+1.37}_{-0.13}$	<0.18
02918	177.412652	22.395723	1.78	2.95 [2.72, 2.91]	25.22	$8.37^{+0.15}_{-0.08}$	$0.10^{+0.34}_{-0.10}$	$8.42^{+0.11}_{-0.14}$	<70.32	$1.25^{+0.72}_{-0.80}$
03746	177.391848	22.400105	1.25	3.78 [3.56, 3.83]	22.48	$8.81^{+0.03}_{-0.01}$	<0.01	$8.11^{+0.10}_{-0.11}$	$10.95^{+1.61}_{-0.58}$	<0.17

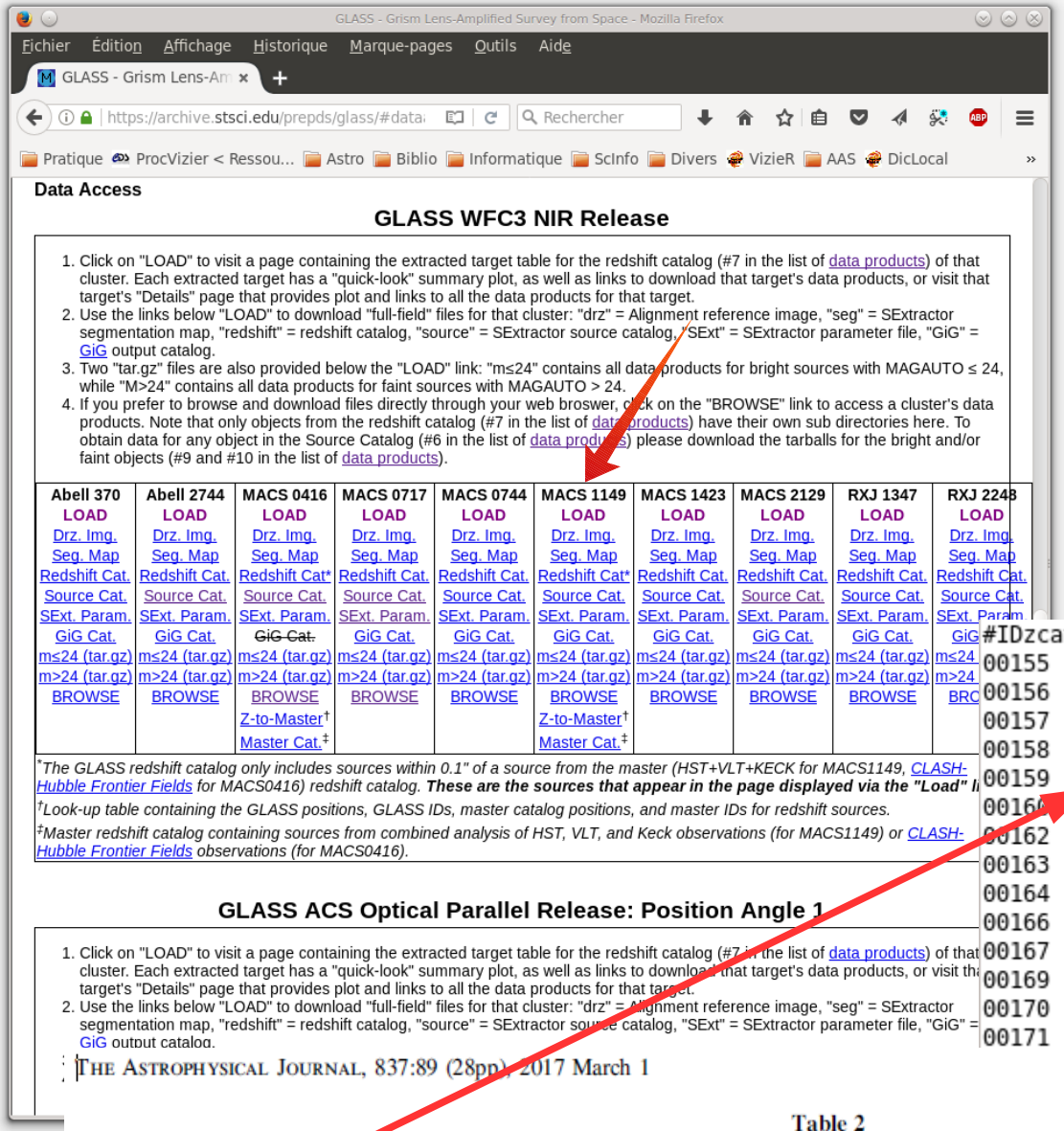

Télécharger les fichiers concernés
Et essayer de retrouver un numéro de la table publiée...

#IDzcat	IDGLASSv001	RA	DEC	redshift	quality	source	
00155	01417	177.413454	22.393843	1.8615	3	1	#
00156	01419	177.416597	22.393925	0.9603	3	1	#
00157	01439	177.390414	22.393626	1.5929	3	1	#
00158	01390	177.408021	22.394379	1.1157	3	1	#
00159	01422	177.386689	22.393877	1.2396	3	1	#
00160	01423	177.400055	22.393982	1.2329	3	1	# 13.3
00162	01305	177.387246	22.394232	2.3195	4	1	#
00163	01301	177.387813	22.395395	0.5432	3	1	#
00164	01414	177.410473	22.394124	1.7084	3	1	#
00166	01388	177.408749	22.394475	2.3189	3	1	# 200.1
00167	01373	177.409808	22.394625	1.2455	3	1	#
00169	01322	177.392541	22.394921	1.4890	3	3	#
00170	01365	177.407378	22.394796	0.5460	4	3	#
00171	00950	177.399831	22.397253	0.5600	4	3	#

Table 2
Global Demographic Properties of the Metallicity Gradient Sample Analyzed in This Work

ID	R.A. (deg.)	Decl. (deg.)	z_{spec}	μ^a	H_{160} Magnitude (ABmag)	SED Fitting		EL Diagnostics		
						$\log(M_*{}^b/M_\odot)$	A_V^{Sc}	$12+\log(O/H)$	SFR^b [$M_\odot$ yr^{-1}]	A_V^{Nc}
01422	177.398643	22.387499	2.28	2.35 [2.09, 2.26]	24.46	$9.29^{+0.07}_{-0.01}$	<0.01	$8.26^{+0.11}_{-0.13}$	$15.10^{+16.76}_{-7.11}$	<1.07
02389	177.406546	22.392860	1.89	43.25 [37.47, 50.28]	23.29	$8.43^{+0.06}_{-0.07}$	<0.01	$7.88^{+0.16}_{-0.15}$	<6.37	$1.36^{+0.69}_{-0.82}$
02607[d]	177.413454	22.393843	1.86	3.01 [2.79, 2.98]	22.63	$10.25^{+0.06}_{-0.10}$	$1.70^{+0.42}_{-0.18}$	$7.70^{+0.13}_{-0.11}$	>36.51	$2.26^{+0.31}_{-0.58}$
02806	177.392541	22.394921	1.50	4.82 [3.11, 3.51]	23.35	$8.72^{+0.19}_{-0.01}$	$0.50^{+0.01}_{-0.01}$	$7.96^{+0.15}_{-0.16}$	$1.96^{+1.37}_{-0.13}$	<0.18
02918	177.412652	22.395723	1.78	2.95 [2.72, 2.91]	25.22	$8.37^{+0.15}_{-0.08}$	$0.10^{+0.34}_{-0.10}$	$8.42^{+0.11}_{-0.14}$	<70.32	$1.25^{+0.72}_{-0.80}$
03746	177.391848	22.400105	1.25	3.78 [3.56, 3.83]	22.48	$8.81^{+0.03}_{-0.01}$	<0.01	$8.11^{+0.10}_{-0.11}$	$10.95^{+1.61}_{-0.58}$	<0.17

GLASS - Grism Lens-Amplified Survey from Space - Mozilla Firefox

Fichier Édition Affichage Historique Marque-pages Outils Aide

GLASS - Grism Lens-Am

https://archive.stsci.edu/prepds/glass/#data Rechercher

Pratique ProcVizier < Ressou... Astro Biblio Informatique ScInfo Divers VizieR AAS DicLocal

Data Access

GLASS WFC3 NIR Release

1. Click on "LOAD" to visit a page containing the extracted target table for the redshift catalog (#7 in the list of data products) of that cluster. Each extracted target has a "quick-look" summary plot, as well as links to download that target's data products, or visit that target's "Details" page that provides plot and links to all the data products for that target.
2. Use the links below "LOAD" to download "full-field" files for that cluster: "drz" = Alignment reference image, "seg" = SExtractor segmentation map, "redshift" = redshift catalog, "source" = SExtractor source catalog, "SExt" = SExtractor parameter file, "GiG" = GiG output catalog.
3. Two "tar.gz" files are also provided below the "LOAD" link: "m≤24" contains all data products for bright sources with MAGAUTO ≤ 24, while "M>24" contains all data products for faint sources with MAGAUTO > 24.
4. If you prefer to browse and download files directly through your web broswer, click on the "BROWSE" link to access a cluster's data products. Note that only objects from the redshift catalog (#7 in the list of data products) have their own sub directories here. To obtain data for any object in the Source Catalog (#6 in the list of data products) please download the tarballs for the bright and/or faint objects (#9 and #10 in the list of data products).

Abell 370	Abell 2744	MACS 0416	MACS 0717	MACS 0744	MACS 1149	MACS 1423	MACS 2129	RXJ 1347	RXJ 2248
LOAD	LOAD	LOAD	LOAD	LOAD	LOAD	LOAD	LOAD	LOAD	LOAD
Drz. Img.	Drz. Img.	Drz. Img.	Drz. Img.	Drz. Img.	Drz. Img.	Drz. Img.	Drz. Img.	Drz. Img.	Drz. Img.
Seg. Map	Seg. Map	Seg. Map	Seg. Map	Seg. Map	Seg. Map	Seg. Map	Seg. Map	Seg. Map	Seg. Map
Redshift Cat.	Redshift Cat.	Redshift Cat*	Redshift Cat.	Redshift Cat.	Redshift Cat*	Redshift Cat.	Redshift Cat.	Redshift Cat.	Redshift Cat.
Source Cat.	Source Cat.	Source Cat.	Source Cat.	Source Cat.	Source Cat.	Source Cat.	Source Cat.	Source Cat.	Source Cat.
SExt. Param.	SExt. Param.	SExt. Param.	SExt. Param.	SExt. Param.	SExt. Param.	SExt. Param.	SExt. Param.	SExt. Param.	SExt. Param.
GiG Cat.	GiG Cat.	~~GiG Cat.~~	GiG Cat.	GiG Cat.	GiG Cat.	GiG Cat.	GiG Cat.	GiG Cat.	GiG
m≤24 (tar.gz)	m≤24 (tar.gz)	m≤24 (tar.gz)	m≤24 (tar.gz)	m≤24 (tar.gz)	m≤24 (tar.gz)	m≤24 (tar.gz)	m≤24 (tar.gz)	m≤24 (tar.gz)	m≤24
m>24 (tar.gz)	m>24 (tar.gz)	m>24 (tar.gz)	m>24 (tar.gz)	m>24 (tar.gz)	m>24 (tar.gz)	m>24 (tar.gz)	m>24 (tar.gz)	m>24 (tar.gz)	m>24
BROWSE	BROWSE	BROWSE	BROWSE	BROWSE	BROWSE	BROWSE	BROWSE	BROWSE	BRO
		Z-to-Master†			Z-to-Master†				
		Master Cat.‡			Master Cat.‡				

*The GLASS redshift catalog only includes sources within 0.1" of a source from the master (HST+VLT+KECK for MACS1149, CLASH-Hubble Frontier Fields for MACS0416) redshift catalog. **These are the sources that appear in the page displayed via the "Load" li**

†Look-up table containing the GLASS positions, GLASS IDs, master catalog positions, and master IDs for redshift sources.

‡Master redshift catalog containing sources from combined analysis of HST, VLT, and Keck observations (for MACS1149) or CLASH-Hubble Frontier Fields observations (for MACS0416).

GLASS ACS Optical Parallel Release: Position Angle 1

1. Click on "LOAD" to visit a page containing the extracted target table for the redshift catalog (#7 in the list of data products) of that cluster. Each extracted target has a "quick-look" summary plot, as well as links to download that target's data products, or visit that target's "Details" page that provides plot and links to all the data products for that target.
2. Use the links below "LOAD" to download "full-field" files for that cluster: "drz" = Alignment reference image, "seg" = SExtractor segmentation map, "redshift" = redshift catalog, "source" = SExtractor source catalog, "SExt" = SExtractor parameter file, "GiG" = GiG output catalog.

Télécharger les fichiers concernés
Et essayer de retrouver un numéro de la table publiée…

#IDzcat	IDGLASSv001	RA	DEC	redshift	quality	source	
00155	01417	177.413454	22.393843	1.8615	3	1	#
00156	01419	177.416597	22.393925	0.9603	3	1	#
00157	01439	177.390414	22.393626	1.5929	3	1	#
00158	01390	177.408021	22.394379	1.1157	3	1	#
00159	01422	177.386689	22.393877	1.2396	3	1	#
00160	01423	177.400055	22.393982	1.2329	3	1	# 13.3
00162	01305	177.387246	22.394232	2.3195	4	1	#
00163	01301	177.387813	22.395395	0.5432	3	1	#
00164	01414	177.410473	22.394124	1.7084	3	1	#
00166	01388	177.408749	22.394475	2.3189	3	1	# 200.1
00167	01373	177.409808	22.394625	1.2455	3	1	#
00169	01322	177.392541	22.394921	1.4890	3	3	#
00170	01365	177.407378	22.394796	0.5460	4	3	#
00171	00950	177.399831	22.397253	0.5600	4	3	#

???

The Astrophysical Journal, 837:89 (28pp), 2017 March 1 Wang et al.

Table 2

Global Demographic Properties of the Metallicity Gradient Sample Analyzed in This Work

ID	R.A. (deg.)	Decl. (deg.)	z_{spec}	μ^a	H_{160} Magnitude (ABmag)	SED Fitting		EL Diagnostics		
						$\log(M_*{}^b/M_\odot)$	A_V^{Sc}	$12+\log(O/H)$	SFR^b [$M_\odot$ yr^{-1}]	A_V^{Nc}
01422	177.398643	22.387499	2.28	2.35 [2.09, 2.26]	24.46	$9.29^{+0.07}_{-0.01}$	<0.01	$8.26^{+0.11}_{-0.13}$	$15.10^{+16.76}_{-7.11}$	<1.07
02389	177.406546	22.392860	1.89	43.25 [37.47, 50.28]	23.29	$8.43^{+0.06}_{-0.07}$	<0.01	$7.88^{+0.16}_{-0.15}$	<6.37	$1.36^{+0.69}_{-0.82}$
02607[d]	177.413454	22.393843	1.86	3.01 [2.79, 2.98]	22.63	$10.25^{+0.06}_{-0.10}$	$1.70^{+0.42}_{-0.18}$	$7.70^{+0.13}_{-0.11}$	>36.51	$2.26^{+0.31}_{-0.58}$
02806	177.392541	22.394921	1.50	4.82 [3.11, 3.51]	23.35	$8.72^{+0.19}_{-0.01}$	$0.50^{+0.01}_{-0.01}$	$7.96^{+0.15}_{-0.16}$	$1.96^{+1.37}_{-0.13}$	<0.18
02918	177.412652	22.395723	1.78	2.95 [2.72, 2.91]	25.22	$8.37^{+0.15}_{-0.08}$	$0.10^{+0.34}_{-0.10}$	$8.42^{+0.11}_{-0.14}$	<70.32	$1.25^{+0.72}_{-0.80}$
03746	177.391848	22.400105	1.25	3.78 [3.56, 3.83]	22.48	$8.81^{+0.03}_{-0.01}$	<0.01	$8.11^{+0.10}_{-0.11}$	$10.95^{+1.61}_{-0.58}$	<0.17

Il faut donc créer un acronyme dédié
ie. mettre à jour :
- le Dictionnaire
- la référence de SIMBAD

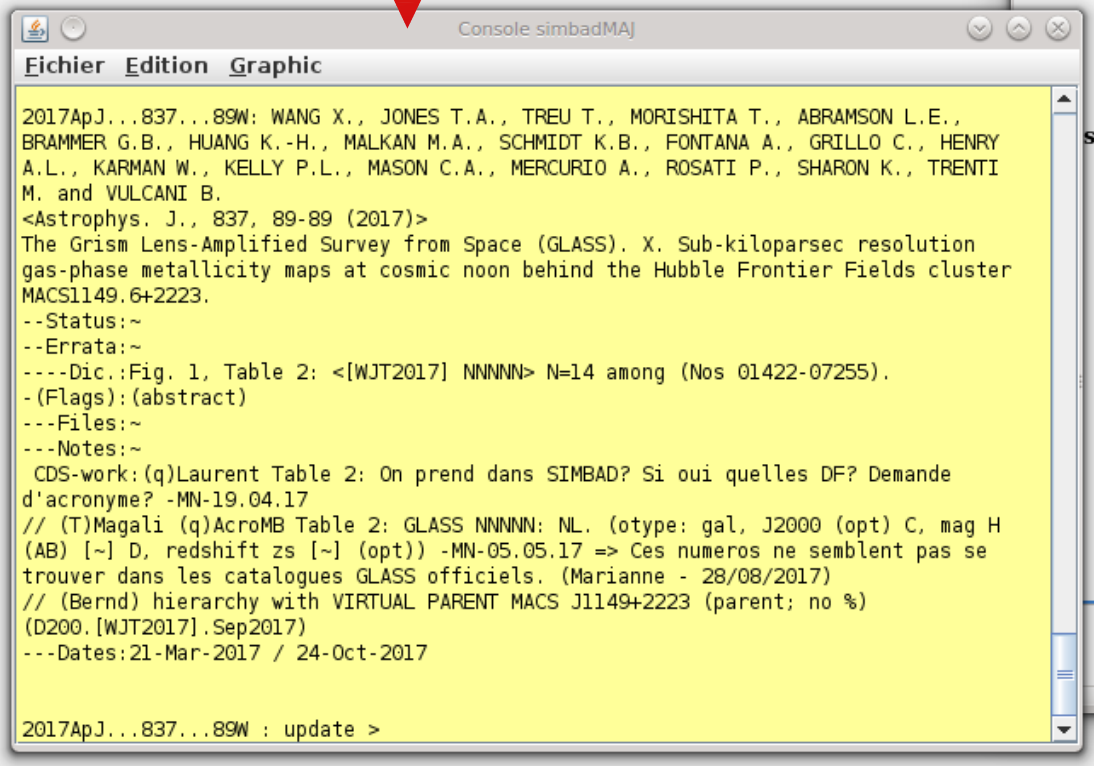

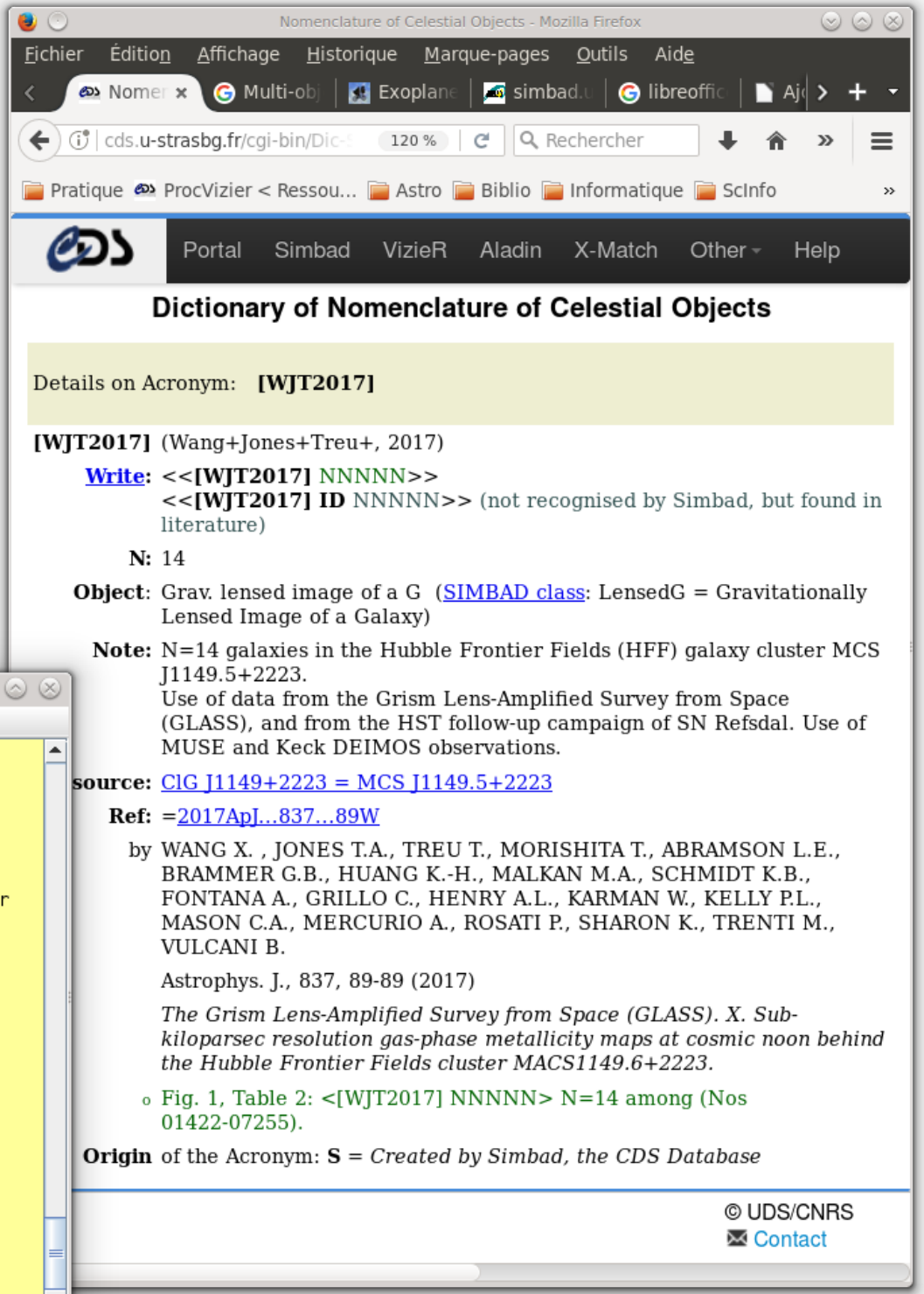

Il faut donc créer un acronyme dédié
ie. mettre à jour :
- le Dictionnaire
- la référence de SIMBAD

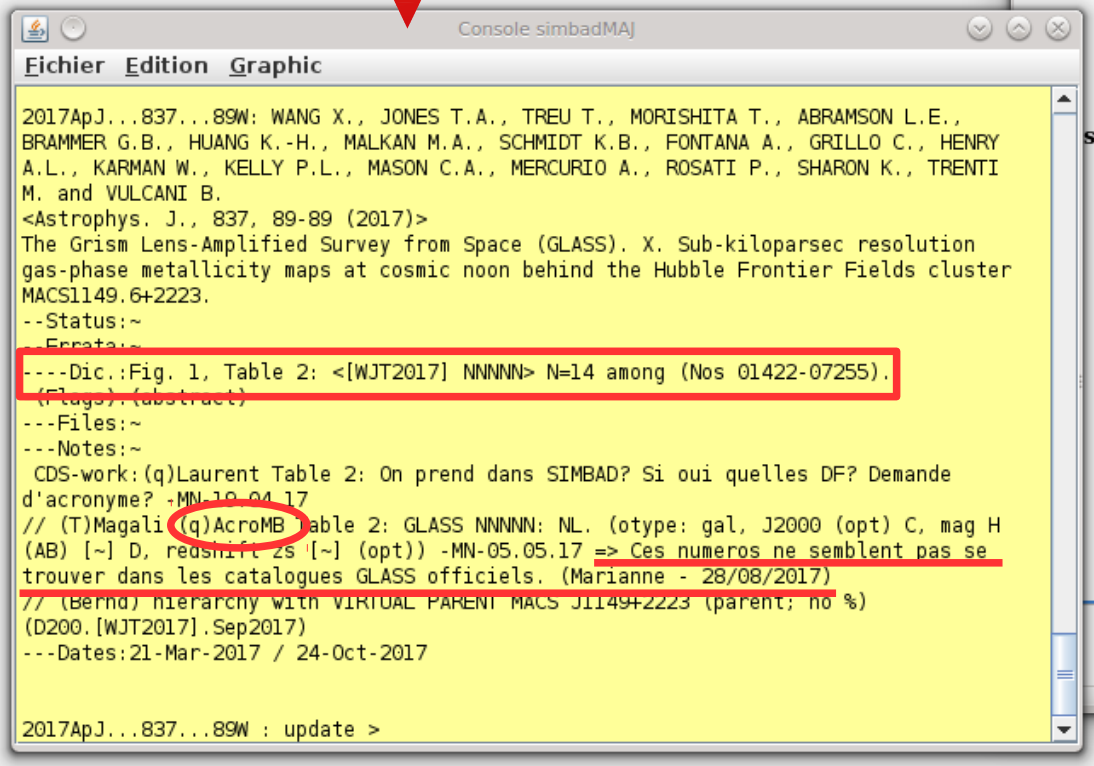

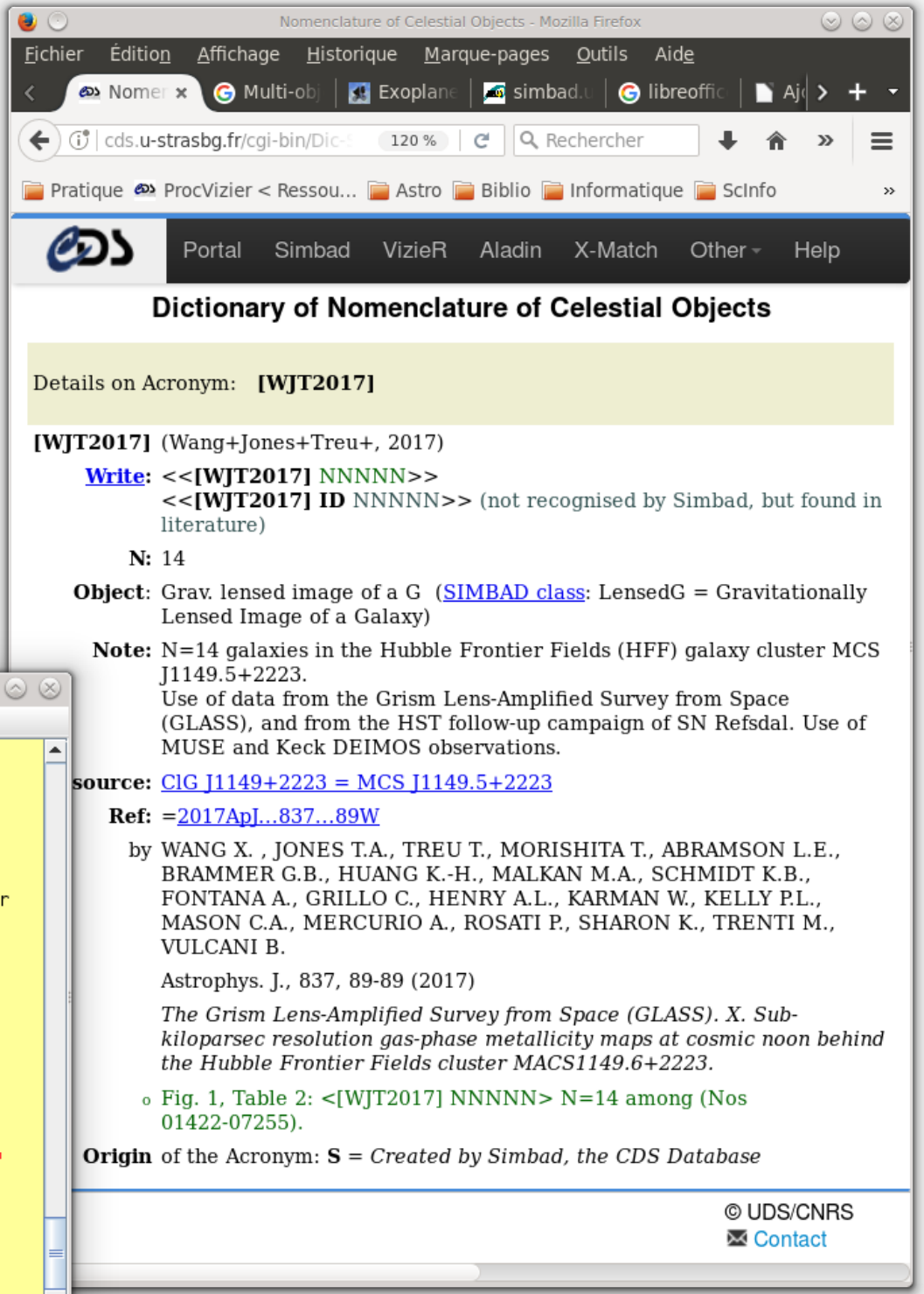

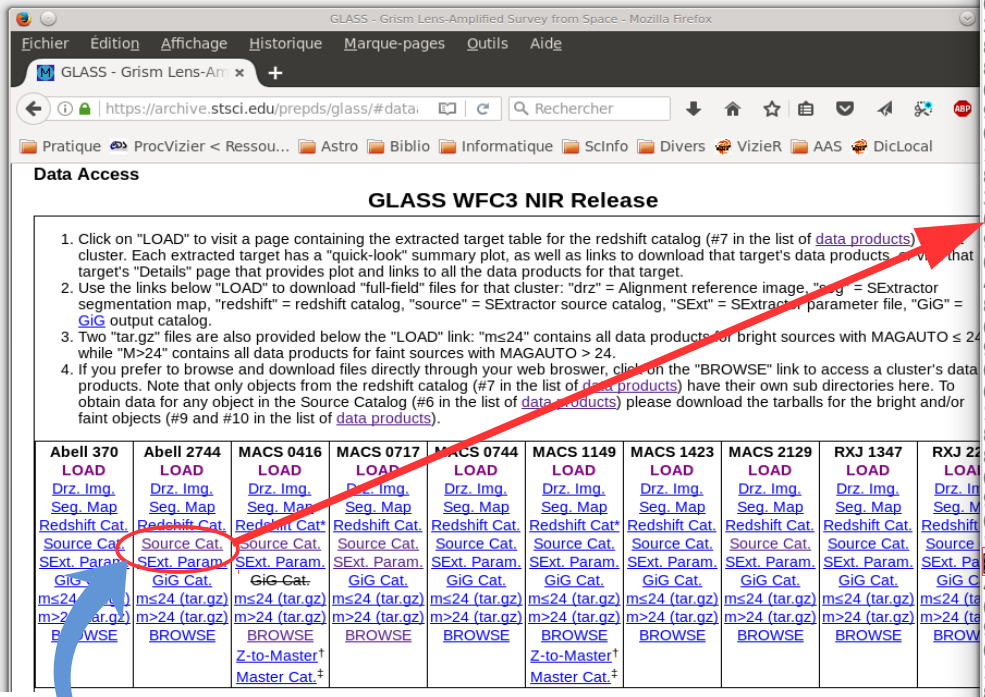

Table 2

$z \gtrsim 7$ Dropout Samples with No Lyα Detection from VI

Cluster	ID GLASS	ID Ancillary	R.A. (degree)	decl. (degree)	P.A. (degree)	Sample	N_{sel}/N_{tot}
A2744	00085	03230	3.593803625	−30.415444323	135, 233	Gold	4/11
A2744	00131	03158	3.570658150	−30.414663281	135, 233	Gold	3/11
A2744	00220	03040	3.592948356	−30.413331741	135, 233	Gold	2/11
A2744	00307	02873	3.585805956	−30.411751960	135, 233	Gold	2/11
A2744	00360[a]	02721	3.603208705	−30.410356491	135, 233	Gold	4/11
A2744	00412	02732	3.600611950	−30.410302069	135, 233	Gold	3/11
A2744	00444[a]	02676	3.592367074	−30.409889954	135, 233	Gold	4/11
A2744	00458	02627	3.604762132	−30.409290304	135, 233	Gold	2/11
A2744	00483	02686	3.596557317	−30.409003929	135, 233	Gold	2/11
A2744	00748	02234	3.580452097	−30.405043370	135, 233	Gold	3/11
A2744	00807	02178	3.600055342	−30.404393062	135, 233	Gold	2/11
A2744	00818	02135	3.601100197	−30.403956945	135, 233	Gold	3/11
A2744	01036	01942	3.567777944	−30.401277987	135, 233	Gold	2/11
A2744	01069	01891	3.601044487	−30.400590602	135, 233	Gold	2/11
A2744	01204[b]	−00088	3.585323923	−30.397960001	135, 233	Gold	3/11
A2744	01335[a]	01506	3.597814977	−30.395957621	135, 233	Gold	3/11
A2744	01929	00847	3.606221824	−30.386645344	135, 233	Gold	2/11
A2744	01972	00816	3.576890999	−30.386328547	135, 233	Gold	3/11
A2744	01992[a]	00765	3.596089446	−30.385830967	135, 233	Gold	4/11
A2744	02040	00723	3.608995192	−30.385282140	135, 233	Gold	3/11
A2744	02157	00557	3.603418234	−30.383215863	135, 233	Gold	3/11
A2744	02193	00477	3.603853194	−30.382264279	135, 233	Gold	3/11
A2744	02199[a]	00469	3.603383290	−30.382256248	135, 233	Gold	4/11
A2744	02204	00479	3.604003006	−30.382306486	135, 233	Gold	2/11
A2744	02209	00487	3.598091105	−30.382391542	135, 233	Gold	2/11
A2744	02266	00433	3.605063809	−30.381462296	135, 233	Gold	3/11
A2744	02283[a]	00600	3.606467680	−30.380994116	135, 233	Gold	4/11
A2744	02295	00599	3.606564953	−30.380917190	135, 233	Gold	3/11
A2744	02317	00333	3.604519959	−30.380466741	135, 233	Gold	5/11
A2744	02379	00265	3.590532446	−30.379764602	135, 233	Gold	2/11
A2744	02428	00163	3.588984152	−30.378668677	135, 233	Gold	3/11
MACS0717	00908	01656	109.377446020	37.743640029	020, 280	Gold	2/13
MACS1423	00684	01408	215.972592500	24.072659477	008, 088	Gold	3/11
MACS1423	01479	00656	215.928811200	24.083905686	008, 088	Gold	3/12
MACS2129	01555	00475	322.373418740	−7.680549573	050, 328	Gold	2/12
MACS2129	01792	00218	322.350848970	−7.675244331	050, 328	Gold	2/12

2, 3, 11	6.96	26.94 ± 0.06	0.40	5.6 ± 1.1	
2, 3	7	27.18 ± 0.07	0.39	4.8 ± 3.4	
2, 3, 4	6.25	27.90 ± 0.07	0.66	3.5 ± 1.4	
3, 4	6.46	27.39 ± 0.16	0.56	2.1 ± 0.9	
1, 3	7.45	27.00 ± 0.06	0.34	2.8 ± 0.8	
2, 3, 11	6.90	27.16 ± 0.07[b]	0.44	3.2 ± 2.8	
2, 3, 11	7	26.58 ± 0.04	0.39	2.9 ± 0.9	
2, 3	5.80	25.98 ± 0.03	1.13	1.7 ± 0.7	
2, 3, 4	6.4	2 ± 0.11	0.57	4.4 ± 7.6	
2, 1, 3, 6	8	0.04	0.30	2.5 ± 5.6	
2, 3, 4	6.10	1.97 ± 0.	1.61	1.5 ± 1.0	
2, 3, 4	5.80	27.69 ± 0.09	1.16	1.7 ± 0.9	
1, 2, 3	8.40	26.91 ± 0.04	0.44	1.6 ± 0.9	
1, 2, 3, 6	8.10	25.82 ± 0.04	0.44	1.6 ± 0.9	
1, 2	8.10	27.74 ± 0.07	0.44	1.6 ± 0.9	
1, 3	7.64	27.79 ± 0.16	0.31	1.8 ± 2.3	
1, 2, 3	7.70	27.99 ± 0.14	0.47	1.5 ± 0.8	
1, 2, 3, 6	7.80	27.09 ± 0.04	0.45	1.5 ± 1.0	
1, 2, 3	7.60	27.07 ± 0.04	0.46	1.5 ± 1.0	
1, 2, 3, 6, 10	8	25.86 ± 0.04	0.44	1.5 ± 0.8	
2, 3	6.10	27.97 ± 0.10	0.76	2.2 ± 1.6	
1, 2, 3	7.89	27.87 ± 0.07	0.44	2.1 ± 1.6	
12, 15	7.25	27.25 ± 0.19	0.44	8.5 ± 19.3	
13, 15, 17	7	27.27 ± 0.19	0.52	...	
11, 15, 17	7	26.14 ± 0.11	0.68	...	
13, 15	7	27.87 ± 0.27	0.44	...	
18, 19	6.85	27.25 ± 0.19	0.12	...	

), 2016 February 10

Y a-t-il d'autres références similaires ?

Oui, plusieurs, comme par exemple 2016ApJ...818...38S

Il faudra là encore un acronyme dédié.

Ces recherches montrent qu'un numéro GLASS était bien donné dans les catalogues existants et dans mes recherches, je suis tombée sur des références utilisant ce "numéro officiel".

Mais il existe déjà un acronyme Glass dans le Dictionnaire…

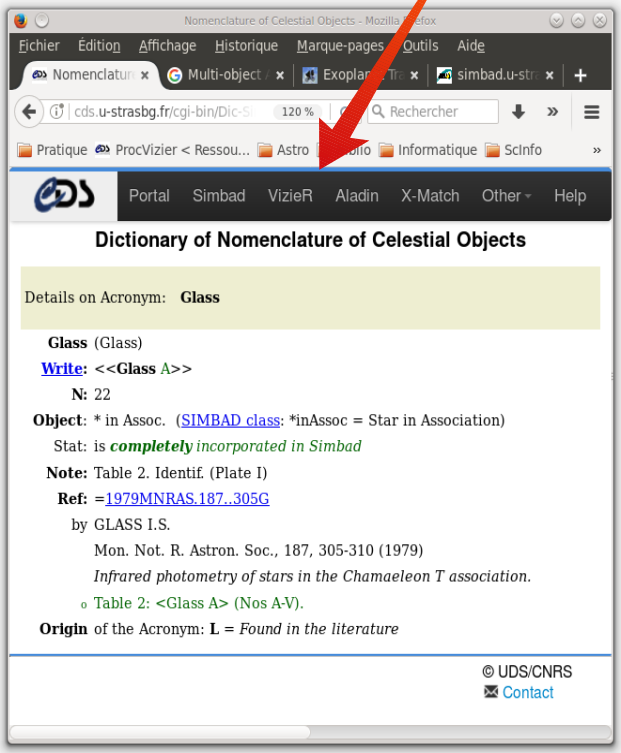

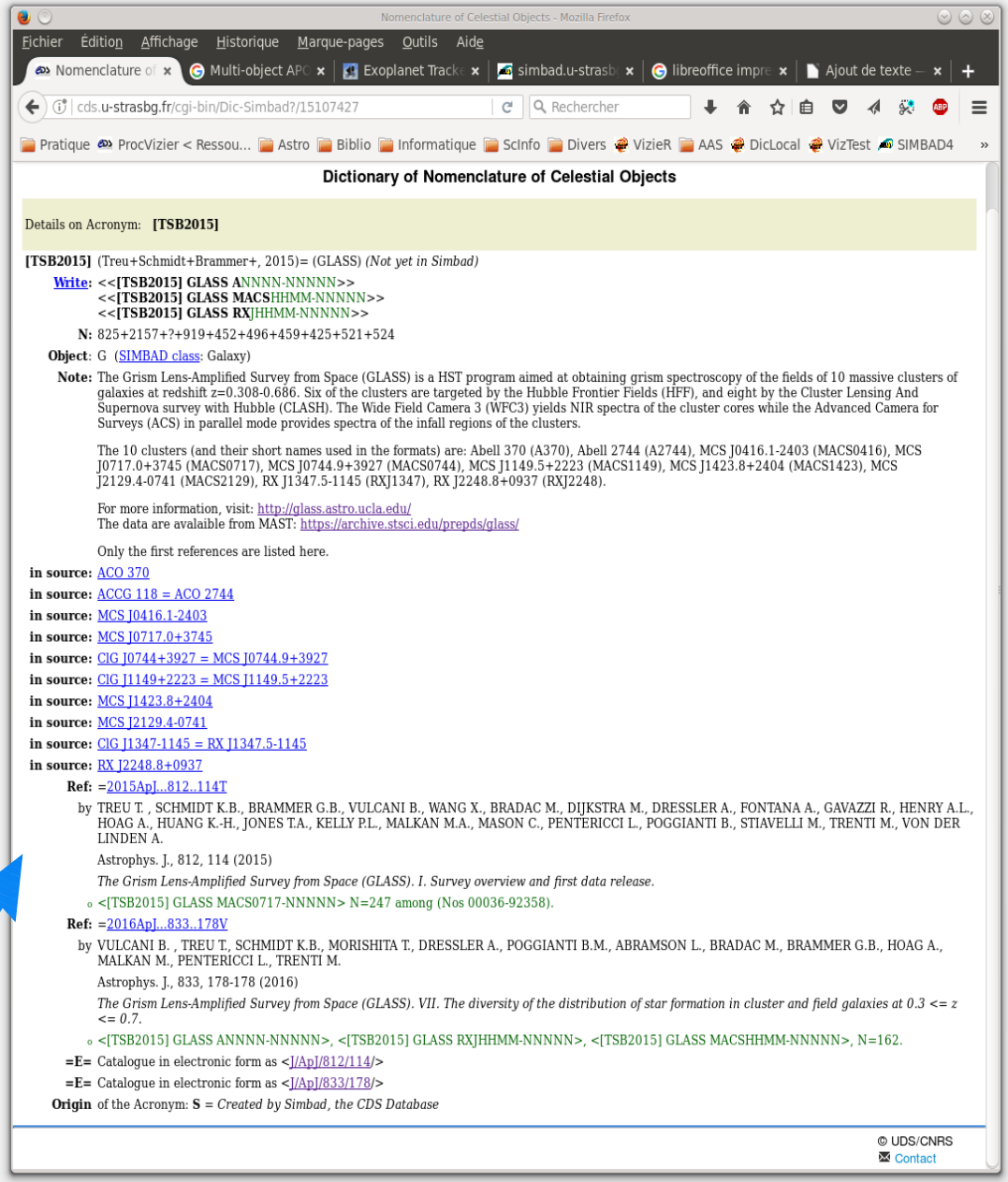

=> J'ai cherché la toute première référence officielle publiée avec ce numéro : elle servira de point de départ.

L'outil du Dictionnaire : DicBuilder

- Anaïs s'occupe de sa maintenance
- Interface graphique permettant de générer le fichier ascii qui constitue le Dictionnaire (19Mo, 876536).

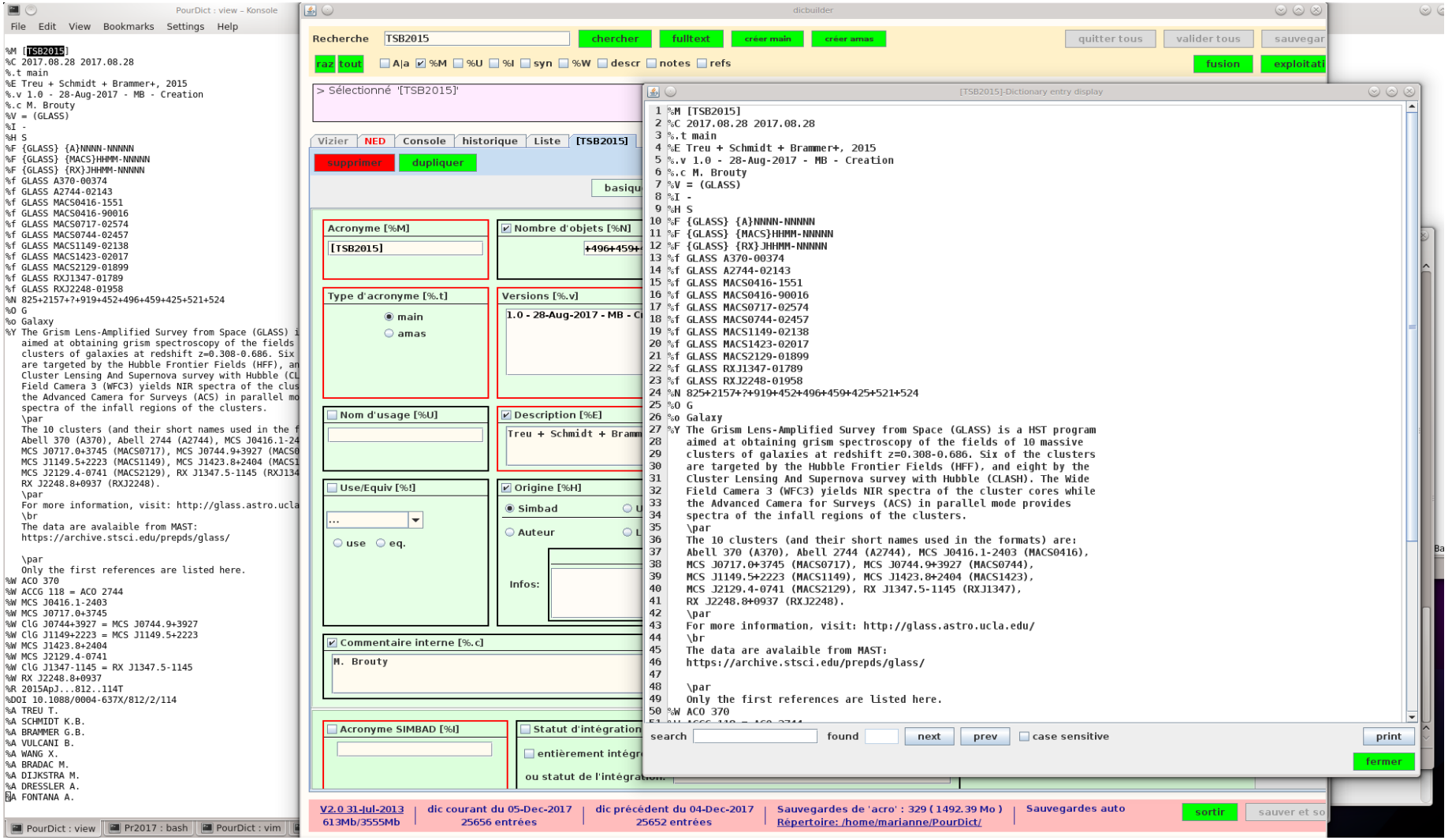

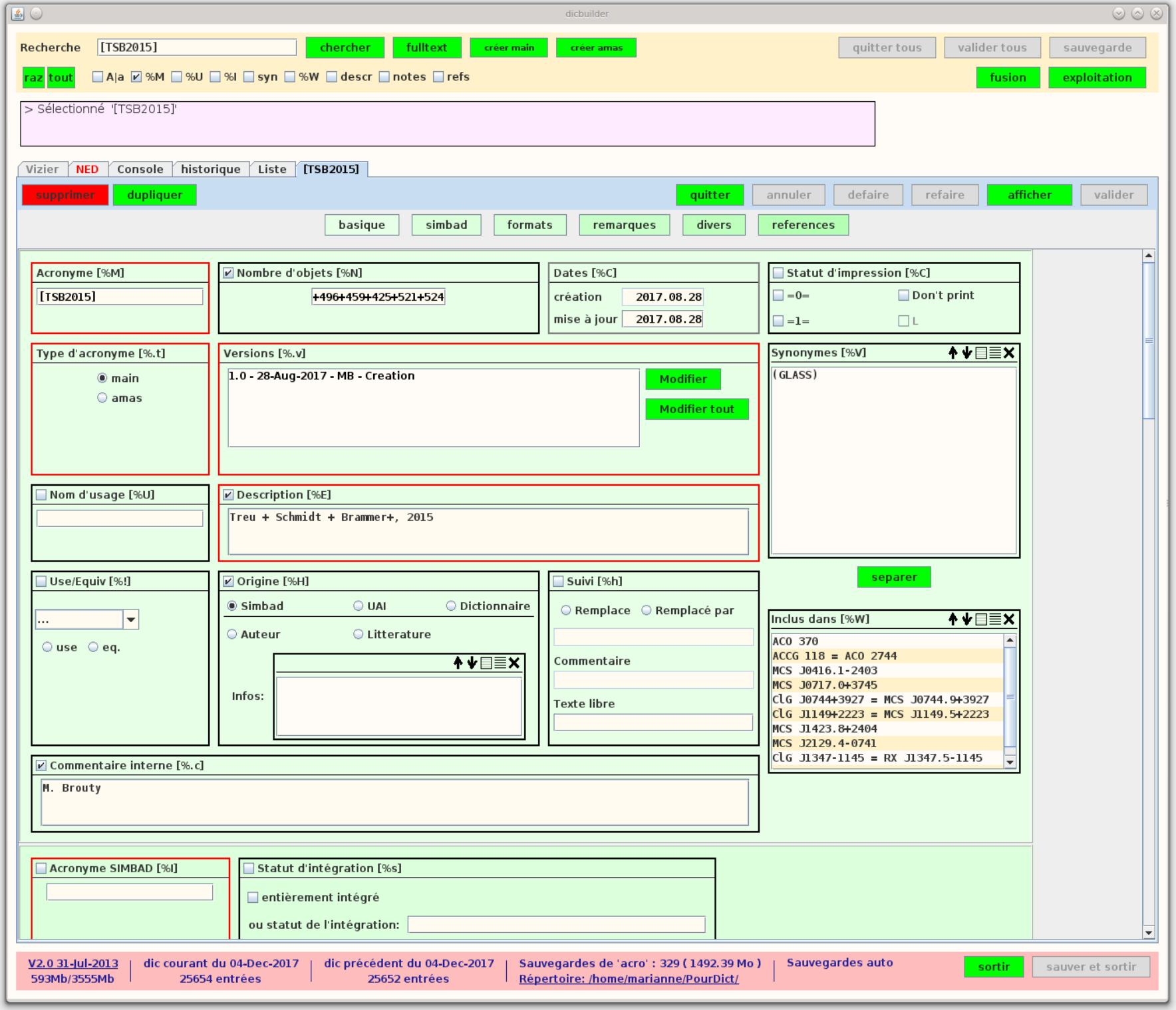
dicbuilder
Recherche
[TSB2015]
chercher
fulltext
créer main
créer amas
quitter tous
valider tous
sauvegarde
raz
tout
A|a
%M
%U
%I
syn
%W
descr
notes
refs
fusion
exploitation
> Sélectionné '[TSB2015]'
Vizier
NED
Console
historique
Liste
[TSB2015]
supprimer
dupliquer
quitter
annuler
defaire
refaire
afficher
valider
basique
simbad
formats
remarques
divers
references
Acronyme [%M]
[TSB2015]
Nombre d'objets [%N]
+496+459+425+521+524
Dates [%C]
création
2017.08.28
mise à jour
2017.08.28
Statut d'impression [%C]
=0=
Don't print
=1=
L
Type d'acronyme [%.t]
main
amas
Versions [%.v]
1.0 - 28-Aug-2017 - MB - Creation
Modifier
Modifier tout
Synonymes [%V]
(GLASS)
Nom d'usage [%U]
Description [%E]
Treu + Schmidt + Brammer+, 2015
séparer
Use/Equiv [%!]
...
use
eq.
Origine [%H]
Simbad
UAI
Dictionnaire
Auteur
Litterature
Infos:
Suivi [%h]
Remplace
Remplacé par
Commentaire
Texte libre
Inclus dans [%W]
ACO 370
ACCG 118 = ACO 2744
MCS J0416.1-2403
MCS J0717.0+3745
ClG J0744+3927 = MCS J0744.9+3927
ClG J1149+2223 = MCS J1149.5+2223
MCS J1423.8+2404
MCS J2129.4-0741
ClG J1347-1145 = RX J1347.5-1145
Commentaire interne [%.c]
M. Brouty
Acronyme SIMBAD [%I]
Statut d'intégration [%s]
entièrement intégré
ou statut de l'intégration:
V2.0 31-Jul-2013
593Mb/3555Mb
dic courant du 04-Dec-2017
25654 entrées
dic précédent du 04-Dec-2017
25652 entrées
Sauvegardes de 'acro' : 329 (1492.39 Mo)
Répertoire: /home/marianne/PourDict/
Sauvegardes auto
sortir
sauver et sortir

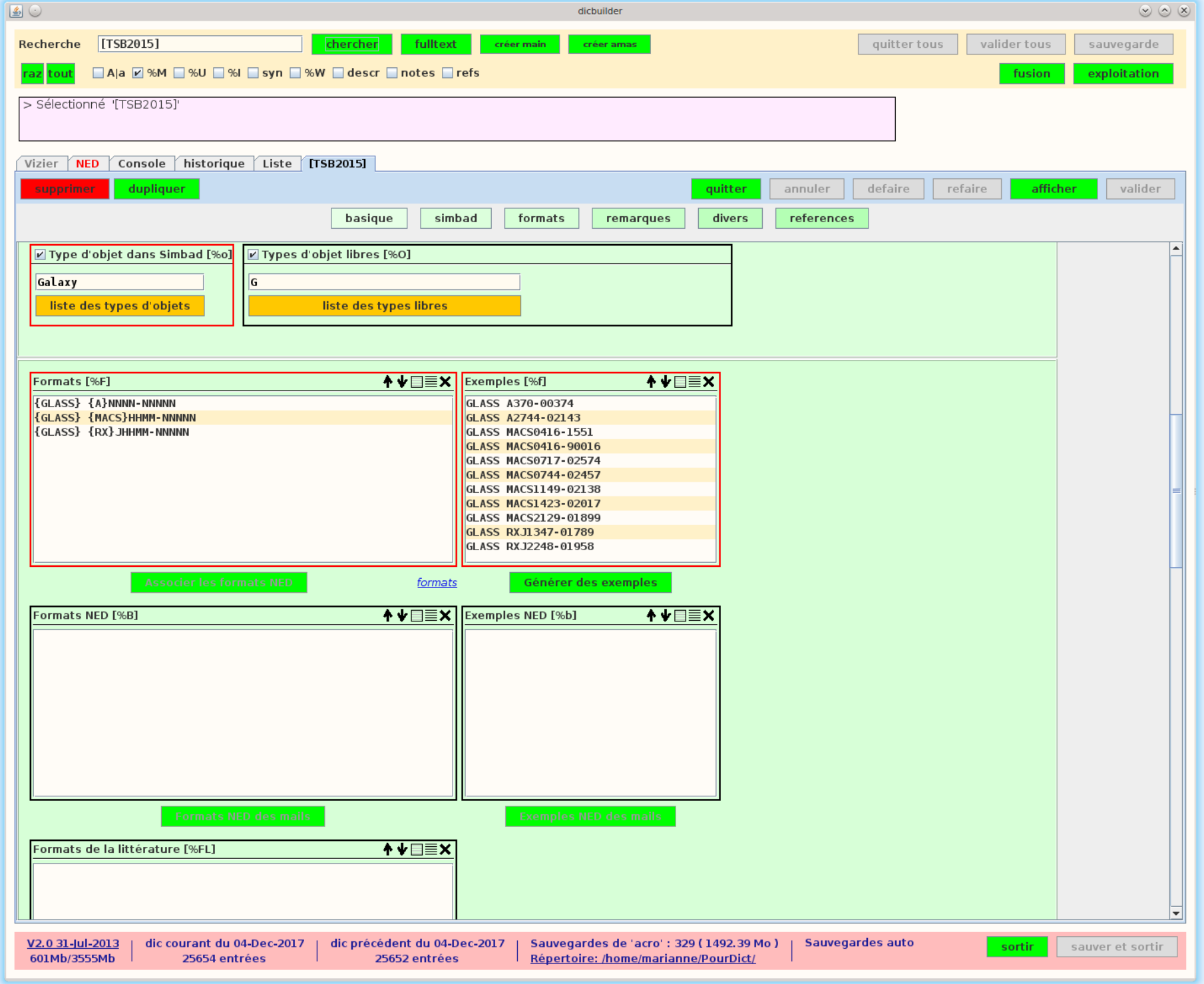
dicbuilder
Recherche
[TSB2015]
chercher
fulltext
créer main
créer amas
quitter tous
valider tous
sauvegarde
raz
tout
A|a
%M
%U
%I
syn
%W
descr
notes
refs
fusion
exploitation
> Sélectionné '[TSB2015]'
Vizier
NED
Console
historique
Liste
[TSB2015]
supprimer
dupliquer
quitter
annuler
defaire
refaire
afficher
valider
basique
simbad
formats
remarques
divers
references
Type d'objet dans Simbad [%o]
Galaxy
liste des types d'objets
Types d'objet libres [%O]
G
liste des types libres
Formats [%F]
{GLASS} {A}NNNN-NNNNN
{GLASS} {MACS}HHMM-NNNNN
{GLASS} {RX}JHHMM-NNNNN
Exemples [%f]
GLASS A370-00374
GLASS A2744-02143
GLASS MACS0416-1551
GLASS MACS0416-90016
GLASS MACS0717-02574
GLASS MACS0744-02457
GLASS MACS1149-02138
GLASS MACS1423-02017
GLASS MACS2129-01899
GLASS RXJ1347-01789
GLASS RXJ2248-01958
Associer les formats NED
formats
Générer des exemples
Formats NED [%B]
Exemples NED [%b]
Formats NED des mails
Exemples NED des mails
Formats de la littérature [%FL]
V2.0 31-Jul-2013
601Mb/3555Mb
dic courant du 04-Dec-2017
25654 entrées
dic précédent du 04-Dec-2017
25652 entrées
Sauvegardes de 'acro' : 329 (1492.39 Mo)
Répertoire: /home/marianne/PourDict/
Sauvegardes auto
sortir
sauver et sortir

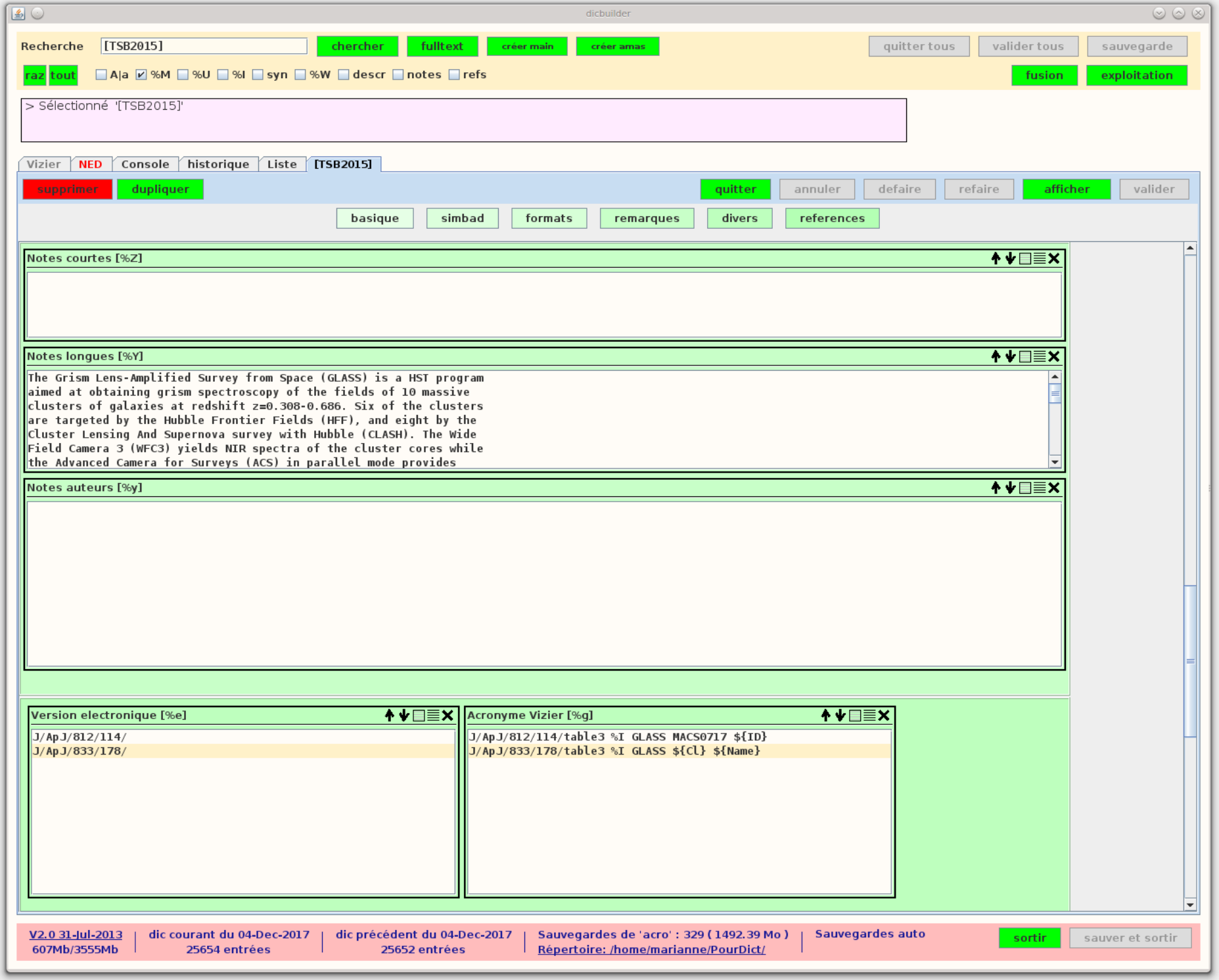
dicbuilder
Recherche
[TSB2015]
chercher
fulltext
créer main
créer amas
quitter tous
valider tous
sauvegarde
raz
tout
A|a
%M
%U
%I
syn
%W
descr
notes
refs
fusion
exploitation
> Sélectionné '[TSB2015]'
Vizier
NED
Console
historique
Liste
[TSB2015]
supprimer
dupliquer
quitter
annuler
defaire
refaire
afficher
valider
basique
simbad
formats
remarques
divers
references
Notes courtes [%Z]
Notes longues [%Y]
The Grism Lens-Amplified Survey from Space (GLASS) is a HST program
aimed at obtaining grism spectroscopy of the fields of 10 massive
clusters of galaxies at redshift z=0.308-0.686. Six of the clusters
are targeted by the Hubble Frontier Fields (HFF), and eight by the
Cluster Lensing And Supernova survey with Hubble (CLASH). The Wide
Field Camera 3 (WFC3) yields NIR spectra of the cluster cores while
the Advanced Camera for Surveys (ACS) in parallel mode provides
Notes auteurs [%y]
Version electronique [%e]
J/ApJ/812/114/
J/ApJ/833/178/
Acronyme Vizier [%g]
J/ApJ/812/114/table3 %I GLASS MACS0717 ${ID}
J/ApJ/833/178/table3 %I GLASS ${Cl} ${Name}
V2.0 31-Jul-2013
607Mb/3555Mb
dic courant du 04-Dec-2017
25654 entrées
dic précédent du 04-Dec-2017
25652 entrées
Sauvegardes de 'acro' : 329 (1492.39 Mo)
Répertoire: /home/marianne/PourDict/
Sauvegardes auto
sortir
sauver et sortir

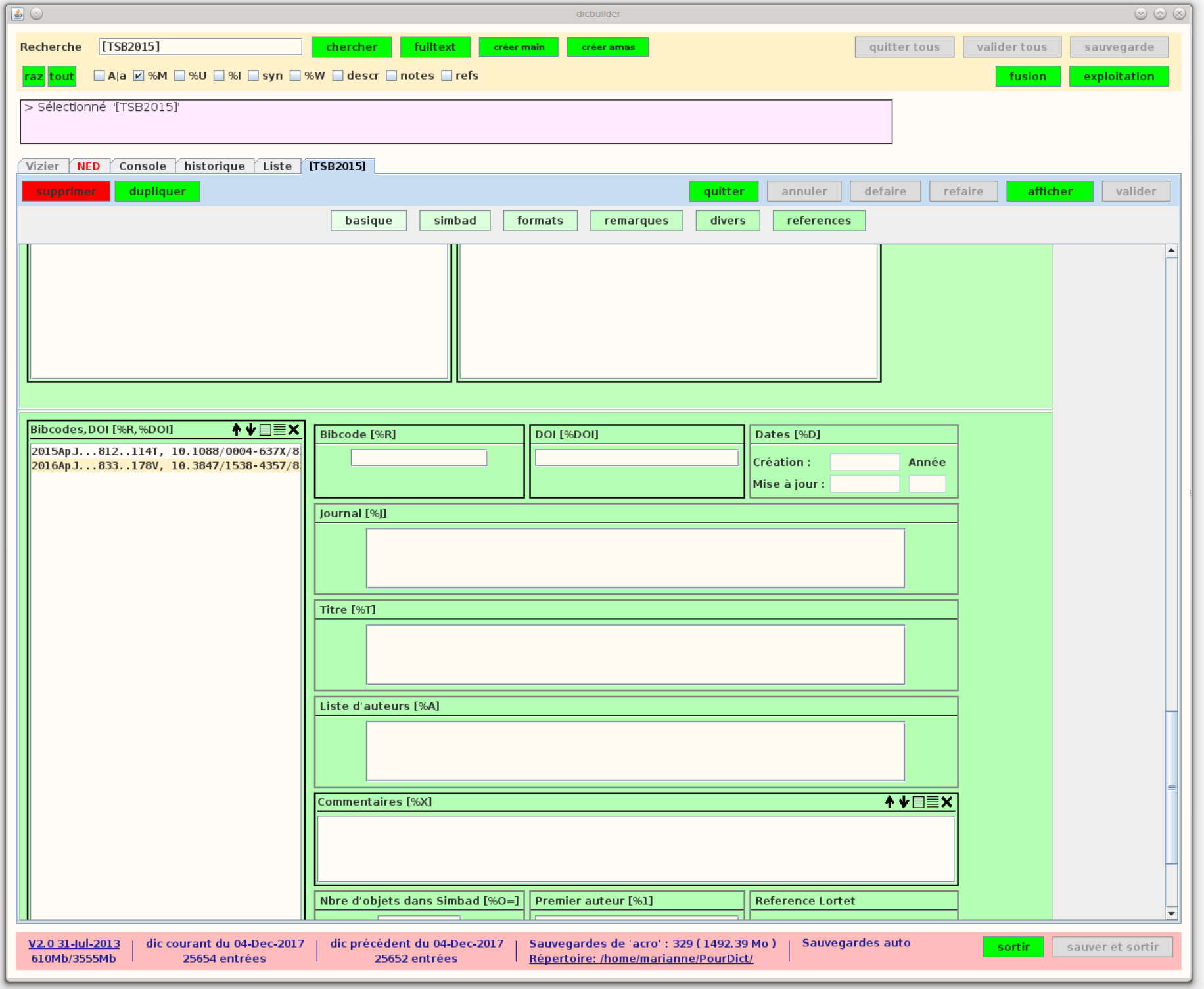
dicbuilder
Recherche
[TSB2015]
chercher
fulltext
créer main
créer amas
quitter tous
valider tous
sauvegarde
raz
tout
A|a
%M
%U
%I
syn
%W
descr
notes
refs
fusion
exploitation
> Sélectionné '[TSB2015]'
Vizier
NED
Console
historique
Liste
[TSB2015]
supprimer
dupliquer
quitter
annuler
defaire
refaire
afficher
valider
basique
simbad
formats
remarques
divers
references
Bibcodes,DOI [%R,%DOI]
2015ApJ...812..114T, 10.1088/0004-637X/8
2016ApJ...833..178V, 10.3847/1538-4357/8
Bibcode [%R]
DOI [%DOI]
Dates [%D]
Création :
Année
Mise à jour :
Journal [%J]
Titre [%T]
Liste d'auteurs [%A]
Commentaires [%X]
Nbre d'objets dans Simbad [%O=]
Premier auteur [%1]
Reference Lortet
V2.0 31-Jul-2013
610Mb/3555Mb
dic courant du 04-Dec-2017
25654 entrées
dic précédent du 04-Dec-2017
25652 entrées
Sauvegardes de 'acro' : 329 (1492.39 Mo)
Répertoire: /home/marianne/PourDict/
Sauvegardes auto
sortir
sauver et sortir

- Utilisation de DJIN pour vérifier la cohérence du Dictionnaire

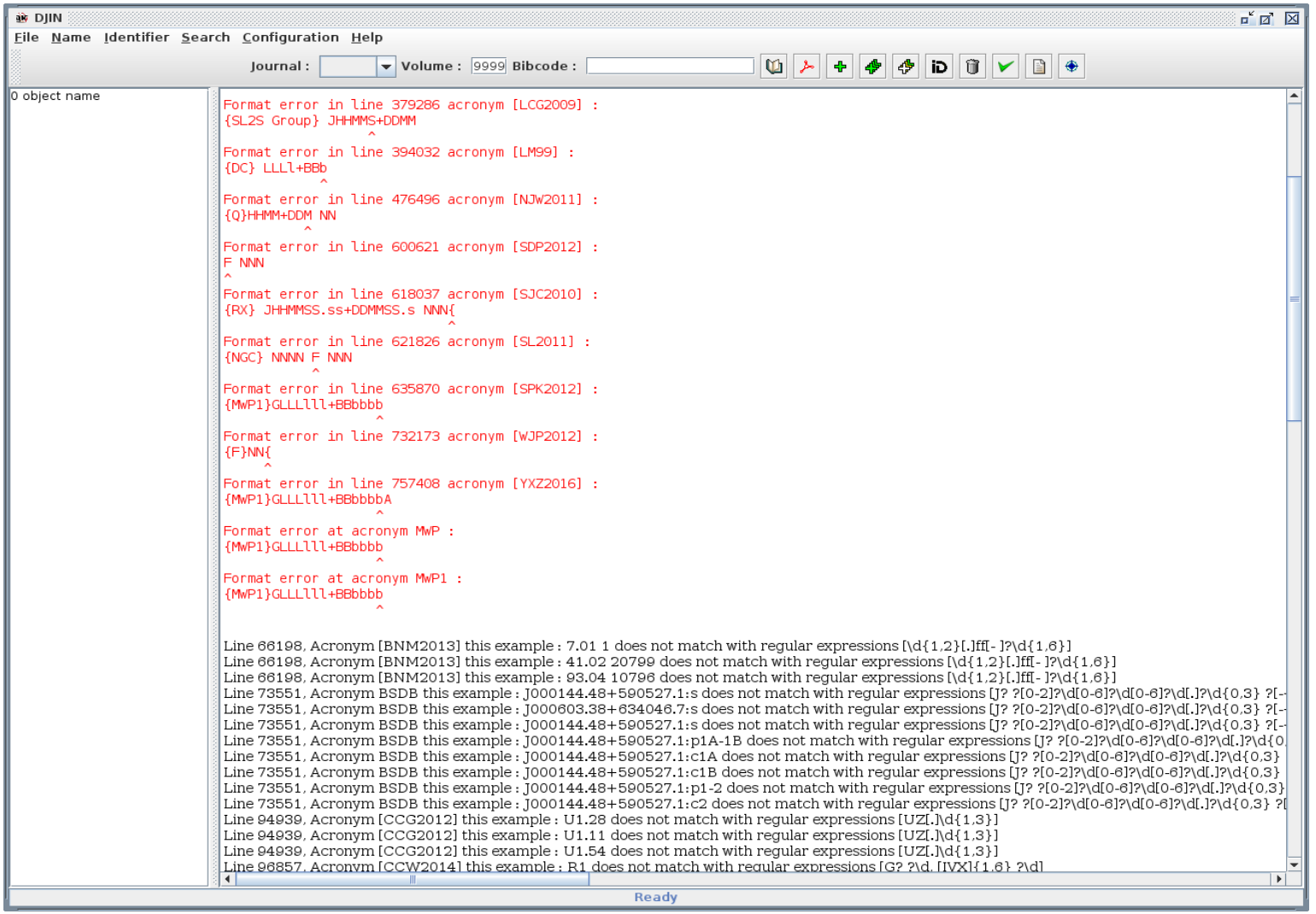

Publication en ligne du Dictionnaire

- Contrairement à SIMBAD, le Dictionnaire est mis à jour localement et publié périodiquement sur le web

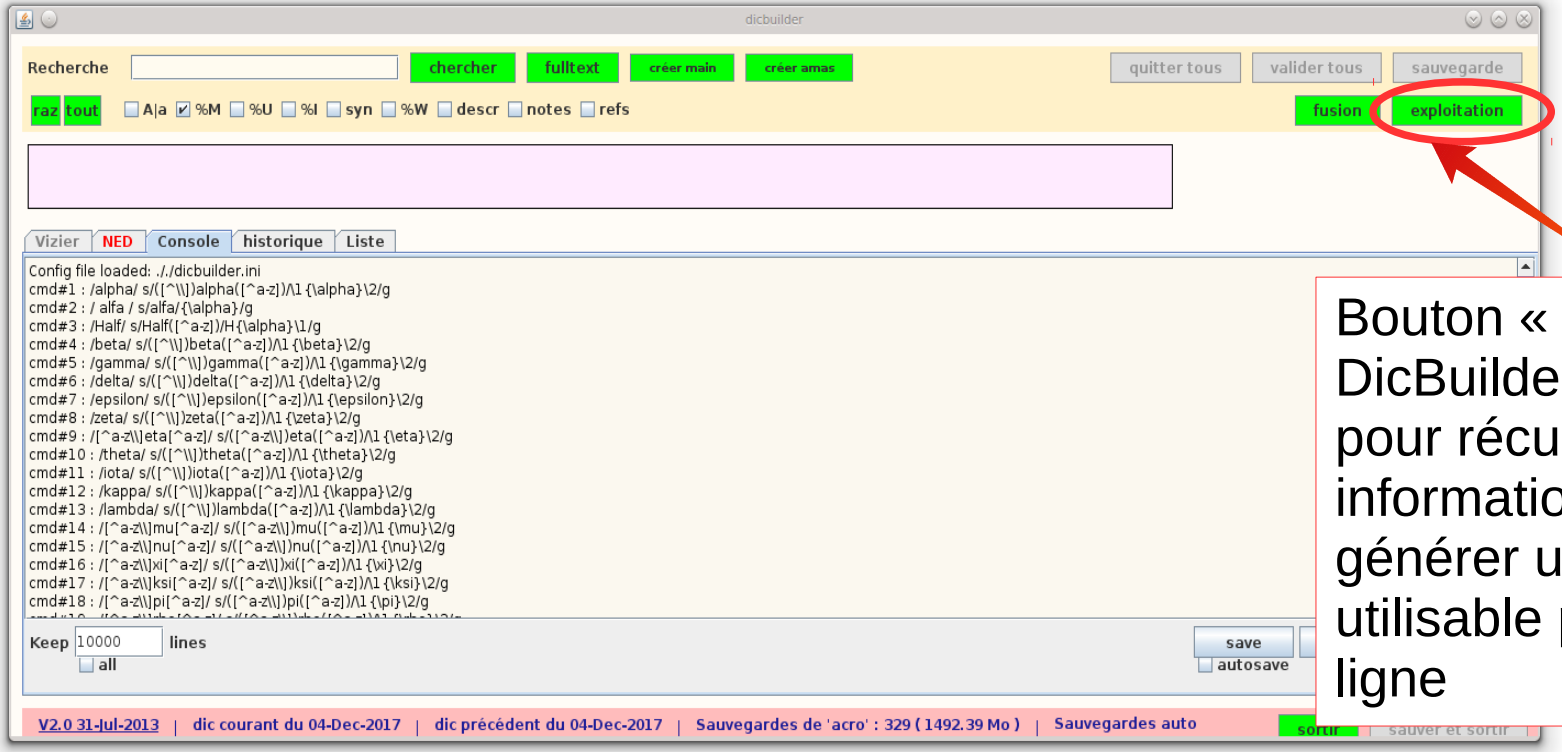

Bouton « exploitation » dans DicBuilder :
pour récupérer les dernières informations de SIMBAD et générer un nouveau fichier utilisable pour la mise en ligne

Puis 2 commandes à lancer depuis un terminal pour mettre cette "nouvelle version" disponible en local puis pour le public